

# Impure AdS/CFT

Sean A. Hartnoll<sup>♭</sup> and Christopher P. Herzog<sup>♯</sup>

<sup>♭</sup> *KITP, University of California  
Santa Barbara, CA 93106-4030, USA*

<sup>♯</sup> *Department of Physics, Princeton University  
Princeton, NJ 08544, USA*

hartnoll@kitp.ucsb.edu, cpherzog@Princeton.EDU

## Abstract

We study momentum relaxation due to dilute, weak impurities in a strongly coupled CFT, a truncation of the M2 brane theory. Using the AdS/CFT correspondence, we compute the relaxation timescale as a function of the background magnetic field  $B$  and charge density  $\rho$ . The theory admits two different types of impurities. We find that for magnetic impurities, momentum relaxation due to the impurity is suppressed by a background  $B$  or  $\rho$ . For electric impurities, due to an underlying instability in the theory towards an ordered phase, the inverse relaxation timescale increases dramatically near  $\sqrt{B^2 + \rho^2/\sigma_0^2} \sim 21T^2$ . We compute the Nernst response for the impure theory, and comment on similarities with recent measurements in superconductors.

# 1 Introduction

Second order quantum phase transitions can occur at zero temperature in condensed matter systems when there is a non-analytic change in the ground state energy as a function of some coupling [1]. On either side of the critical point, at sufficiently low temperatures the system admits a quasiparticle description. The nature of the quasiparticles depends on the orders characterising the different phases. For instance, Néel ordered phases have spin wave excitations whereas phases with Valence Bond Solid order have spinon and ‘photon’ excitations [2]. However, as the temperature is increased, near to the critical coupling, thermal fluctuations lead to competition between the different orders. In this strongly coupled regime, in which both quantum and thermal fluctuations play an important role, neither quasiparticle description is appropriate. Instead the system is best described by a finite temperature 2+1 dimensional conformal field theory (CFT) [1, 2]. Often this theory turns out to be relativistically invariant (the ‘speed of light’ in these theories is not  $c$  but rather some lower speed characterising the material).

Quantum critical points are believed to be important in various systems of experimental interest, including the high  $T_c$  cuprate superconductors [3, 4]. In contrast, the theorist’s toolkit of tractable 2+1 CFTs has largely been limited to the  $O(N)$  model at large  $N$ , and related models with relevant quartic interactions [1, 2]. The AdS/CFT correspondence [5] provides a wealth of new examples of 2+1 CFTs in which explicit computations are possible at large  $N$ . Although this correspondence has been intensely studied for a decade, potential applications to concrete condensed matter systems have only recently begun to be explored [6, 7, 8, 9]. Relevant earlier work on finite temperature physics in  $AdS_4$  includes [10, 11, 12]. Most immediately these CFTs provide new solvable toy models for strongly coupled dynamics in 2+1 dimensions. In the future it might be possible to engineer the relevant supersymmetric CFTs in a lab. One can thus speculate that in addition to having interesting physical properties in their own right, these systems open up the possibility of doing experimental quantum gravity via the AdS/CFT correspondence.

In many experimental systems, microscopic impurities in the samples leave a significant imprint on the physics. Most directly, the impurities are at fixed (random) locations and therefore break translational invariance. This loss leads to a relaxation of momentum at late times. Momentum relaxation is characterised by a timescale  $\tau_{\text{imp}}$ , which will be the main focus of this paper. In many contexts, see e.g. [8] for a discussion, momentum relaxation is necessary for dc ( $\omega = 0$ ) transport to be finite; otherwise the ‘Drude peak’ becomes a delta function as  $1/\tau_{\text{imp}} \rightarrow 0$ . We will exhibit similar ‘metallic’ behaviour in a strongly coupled CFT with impurities.

Given a theory, the effect of impurities can in principle be computed microscopically. One would like to know how the impurity timescale depends on temperature, background magnetic field and charge density. To our knowledge there is no first principles computation of  $\tau_{\text{imp}}(T, B, \rho)$  available in the literature. If the impurities are sufficiently dilute and furthermore weak enough for their interaction with the CFT to be treated perturbatively, then  $\tau_{\text{imp}}$  can be computed from a two point function in the finite temperature CFT. We will derive the formula for  $\tau_{\text{imp}}$  and use the AdS/CFT correspondence to compute it for a truncation of the M2 brane theory.

In sections 2 and 3 we give a general description of the effect of dilute, weak impurities in a CFT. The main result of these sections is equation (12), which expresses the impurity relaxation timescale in terms of the retarded Green’s function of a relevant scalar operator in the theory which couples to the impurities.

In section 4, we show how this Green’s function may be evaluated in a truncation of the M2

brane theory using the AdS/CFT correspondence. Our truncation is not consistent. We neglect a coupling between the scalar and pseudoscalar modes we keep and a second gauge field. The inconsistent truncation is made to keep the calculations simple and also because we have no good physical interpretation of the second gauge field in our condensed matter context. In another small abuse of the M2 brane theory, we give our pseudoscalar operator conformal dimension one instead of two. This gives us a larger collection of relevant operators to study. Note however that the standard M2 brane theory is obtainable as a double trace deformation of ours [13].

In the following section 5 we give our (numerical) results for  $\tau_{\text{imp}}(T, B, \rho)$ . We first note that there are in fact two relevant operators in the theory, dual to linear combinations of the scalar and pseudoscalar of the bulk, with considerably different effects. The operators can be distinguished by their transformation properties under charge conjugation  $\mathcal{C}$ , parity  $\mathcal{P}$ , and time reversal  $\mathcal{T}$ . In the presence of a background magnetic field and finite charge density, the first operator,  $\mathcal{O}_+$ , transforms the same way as the magnetic field while  $\mathcal{O}_-$  transforms as the electric field. We are thus tempted to identify  $\mathcal{O}_+$  with magnetic impurities and  $\mathcal{O}_-$  with electric impurities.

For both operators, we find that the impurity time  $1/\tau_{\text{imp}}$  depends on the charge density  $\rho$  and magnetic field  $B$  only in the combination  $\sqrt{B^2 + \rho^2/\sigma_0^2}$  where  $\sigma_0$  is the electrical conductivity at  $\rho = B = 0$ . This combined dependence, while remarkable, may be an accident of the details of the M2 brane theory.

For the  $\mathcal{O}_+$  impurities, we find that increasing the magnetic field or charge density suppresses momentum relaxation due to impurities. At the same time, at nonzero  $B$  there is an independent source of momentum relaxation due to hydrodynamic cyclotron motion. Increasing  $B$  increases the momentum relaxation due to cyclotron motion.

However, for the other operator,  $\mathcal{O}_-$ , momentum relaxation becomes faster with increasing  $B$  or  $\rho$ . When  $\sqrt{B^2 + \rho^2/\sigma_0^2}$  reaches a critical value of about  $21T^2$ , then  $1/\tau_{\text{imp}} \rightarrow \infty$ . We will see that this divergence is symptomatic of an underlying instability of the theory towards an ordered phase. From a gravitational point of view, the instability occurs when the scalar field dual to  $\mathcal{O}_-$  develops an unstable mode. This instability provides a clean counterexample to the original version of the Gubser-Mitra ‘correlated stability conjecture’ [15, 16], similar to those discussed in [17].

In section 6 we use our results to compute the Nernst coefficient in the CFT. We note that our plots show some qualitative similarities to the organic superconductors studied in [18], perhaps indicating a nearby quantum critical point in that system. While the organic superconductors effectively have vanishing charge density,  $\rho = 0$ , because they are not doped, in the cuprate superconductors the doping  $x$  can be thought of as a nonzero charge density [8].

## 2 The effect of random disorder

The presence of impurities breaks the translational and conformal invariance of the CFT. Locally the impurities will source relevant operators and potentially drive the theory away from the fixed point. Thus we can model the impurities by adding the following coupling to the Hamiltonian

$$\delta H = \int d^2y V(y) \mathcal{O}(t, y). \quad (1)$$

The operator  $\mathcal{O}(t, y)$  is the most relevant operator in the conformal field theory that preserves the global symmetries of the theory. Charged impurities are also of interest, although we shall only study neutral impurities here. This term breaks translation invariance, because the potential  $V(y)$

is explicitly space dependent, and is hard to work with directly. To get around this one treats the impurity potential statistically. If the impurities are sufficiently dilute that their effects do not overlap, then the precise weighting on the space of potentials is not important, and it is useful to take the Gaussian [19]

$$\langle \cdots \rangle_{\text{imp}} = \int \mathcal{D}V e^{-\int d^2y V(y)^2 / 2\bar{V}^2} (\cdots), \quad (2)$$

which implies

$$\langle V(x) \rangle_{\text{imp}} = 0, \quad \langle V(x)V(y) \rangle_{\text{imp}} = \bar{V}^2 \delta^{(2)}(x-y). \quad (3)$$

We will furthermore make the approximation that scattering off impurities may be treated perturbatively, so that we can expand in powers of  $V$ . The strength of the potential  $\bar{V}$  is a dimensionful quantity, with mass dimension

$$[\bar{V}] = 2 - \Delta_{\mathcal{O}}. \quad (4)$$

So long as  $2 - \Delta_{\mathcal{O}} > 0$ ,  $\bar{V}$  has positive scaling dimension and the impurities are a relevant perturbation. This condition that  $\bar{V}$  has positive scaling dimension is often called the Harris criterion [20]. In the case of the M2 brane theory, the most relevant neutral operators are mass terms for the scalar fields [21, 22, 23]. By ‘neutral’ we mean with respect to a certain  $U(1) \subset SO(8)$ , as we describe below. These operators have conformal dimension  $\Delta_{\mathcal{O}} = 1$ . We can anticipate that the relevance of these operators implies that they will become strongly coupled at low energies. We will be careful to keep track of the regime in which perturbation theory in  $\bar{V}$  is valid.

The breaking of translation invariance leads to the late time non conservation of momentum. The timescale associated with the loss of momentum is called the impurity relaxation timescale and is given to leading order in strength of the impurity potential,  $V$ , by

$$\frac{1}{\tau_{\text{imp}}} = -\frac{1}{\chi_0} \lim_{\omega \rightarrow 0} \frac{\text{Im } G_{\mathcal{FF}}^R(\omega, 0)}{\omega}. \quad (5)$$

This equation follows from considering the ‘memory function’. We give a derivation in the following section, along with a discussion of the precise meaning of  $\tau_{\text{imp}}$  and of regimes of validity. To fix conventions, we define the retarded Green’s function of any operator  $\mathcal{O}$  in Fourier space to be

$$G_{\mathcal{OO}}^R(\omega, k) = -i \int d^2x \int_0^\infty dt \langle [\mathcal{O}(t, x), \mathcal{O}(0, 0)] \rangle e^{i\omega t - ik \cdot x}. \quad (6)$$

The quantities that appear in (5) are firstly

$$\chi_0 \equiv \lim_{\omega \rightarrow 0} G_{\mathcal{PP}}^R(\omega, 0) = \epsilon + P, \quad (7)$$

where  $\mathcal{P}$  is the momentum density in a fixed direction, i.e.  $\mathcal{P} = n_i T^{0i}$  for some unit vector  $n \in \mathbb{R}^2$ . The number  $\chi_0$  is the static susceptibility for the momentum density,  $\epsilon$  is the energy density and  $P$  the pressure. The remaining term in (5) is the Green’s function for the operator

$$\mathcal{F}(t, x) = [\mathcal{P}(t, x), \delta H] = \int d^2y V(y) [\mathcal{P}(t, x), \mathcal{O}(t, y)]. \quad (8)$$

This expression simplifies using that the spatial integral of  $\mathcal{P}(t, x)$  is a momentum and hence generates translations. Locally therefore  $[\mathcal{P}(t, x), \mathcal{O}(t, y)] = i\delta^{(2)}(x-y)\partial\mathcal{O}(t, y)$  up to a total derivative with respect to  $x$ . We shall ignore this total derivative; one can use translation invariance to show that this derivative does not contribute to the Green’s function  $G_{\mathcal{FF}}^R$ . Thus (8) becomes

$$\mathcal{F}(t, x) = i \int d^2y V(y) \delta^{(2)}(x-y) \partial\mathcal{O}(t, y) = iV(x) \partial\mathcal{O}(t, x). \quad (9)$$

Here  $\partial$  denotes spatial derivative in the same direction as  $\mathcal{P}$ , i.e.  $\partial = n^i \partial_i$ .

The Green's function is therefore

$$G_{\mathcal{F}\mathcal{F}}^R(\omega, 0) = i\bar{V}^2 \int_0^\infty dt \langle [\partial \mathcal{O}(t, 0), \partial \mathcal{O}(0, 0)] \rangle e^{i\omega t}, \quad (10)$$

where we used (3). Passing to momentum space, one obtains

$$G_{\mathcal{F}\mathcal{F}}^R(\omega, 0) = -\frac{\bar{V}^2}{2} \int \frac{d^2 k}{(2\pi)^2} k^2 G_{\mathcal{O}\mathcal{O}}^R(\omega, k). \quad (11)$$

The factor of 1/2 arises because the integral with  $(n \cdot k)^2$  in the integrand is half the integral with  $k^2$ , by isotropy. Thus

$$\boxed{\frac{1}{\tau_{\text{imp}}} = \frac{\bar{V}^2}{2\chi_0} \lim_{\omega \rightarrow 0} \int \frac{d^2 k}{(2\pi)^2} k^2 \frac{\text{Im} G_{\mathcal{O}\mathcal{O}}^R(\omega, k)}{\omega}}. \quad (12)$$

This is the formula we will use to compute the relaxation timescale  $\tau_{\text{imp}}$ . We will obtain the dependence on charge density  $\rho$  and background magnetic field  $B$ . Due to conformal invariance and dimensional analysis, one has the scaling form

$$\frac{1}{\tau_{\text{imp}}} = \frac{\bar{V}^2}{T^{3-2\Delta_{\mathcal{O}}}} F\left(\frac{\rho}{T^2}, \frac{B}{T^2}\right). \quad (13)$$

### 3 The impurity timescale

#### 3.1 Impurity in the absence of a magnetic field

In this section we derive the expression (5) for the impurity timescale. First note that from the definition of the retarded Green's function, and (twice) using the Heisenberg equation of motion one obtains

$$\omega^2 G_{\mathcal{P}\mathcal{P}}^R(\omega, k) = -G_{[\mathcal{P}, H][\mathcal{P}, H]}^R(\omega, k) + G_{[\mathcal{P}, H][\mathcal{P}, H]}^R(0, k). \quad (14)$$

This equation is true up to contact terms for any operator. In the absence of the impurity potential,  $\mathcal{P}$  is the conserved momentum density as well as the energy current. If we split the total Hamiltonian as  $H = H_0 + \delta H$ , with  $\delta H$  given by (1) above, then  $H_0$  is the Hamiltonian of a translationally invariant theory while  $\delta H$  explicitly breaks this symmetry. It follows that  $[\int d^2 x \mathcal{P}(x), H_0] = 0$ . Thus from the definition of the retarded Green's function, at zero spatial momentum we have that  $G_{[\mathcal{P}, H_0]\mathcal{O}}^R(\omega, 0) = 0$ , for any operator  $\mathcal{O}$ . It follows that

$$\omega^2 G_{\mathcal{P}\mathcal{P}}^R(\omega, 0) = -\left(G_{\mathcal{F}\mathcal{F}}^R(\omega, 0) - G_{\mathcal{F}\mathcal{F}}^R(0, 0)\right). \quad (15)$$

Evaluated in a background with a nonzero  $\bar{V}$ , this result for  $G_{\mathcal{P}\mathcal{P}}^R$  is exact. For us the usefulness of this expression lies in the fact that a  $\bar{V}^2$  trivially factors out of the right hand side, see equation (10), allowing us to evaluate the remainder in a background with vanishing  $\bar{V}$ , thus yielding a result for  $G_{\mathcal{P}\mathcal{P}}^R$  that is accurate to leading order in  $\bar{V}^2$ .

Given this formula (15),  $\lim_{\bar{V} \rightarrow 0} G_{\mathcal{P}\mathcal{P}}^R(\omega, 0) = 0$  as required by the restoration of translational invariance in this limit. However, we have no guarantee that at fixed nonzero  $\bar{V}$  the  $\lim_{\omega \rightarrow 0} G_{\mathcal{P}\mathcal{P}}^R(\omega, 0)/\omega$ , which is proportional to a dc thermal conductivity, is finite. Yet physically, we expect the system with impurities to be well behaved in response to low frequency perturbations. These considerations suggest that the response of the system is governed by a modified Green's function where a contact term has been subtracted:

$$i\theta(\omega, 0)T\omega \equiv G_{\mathcal{P}\mathcal{P}}^R(\omega, 0) - \chi_0. \quad (16)$$

The quantity  $\theta(\omega, 0)$  might be called a momentum conductivity; in appendix A we show that indeed  $\langle \mathcal{P} \rangle = -\theta(\omega, 0) \nabla T$ . By  $\theta$  we mean a diagonal component of the conductivity matrix; there is no off-diagonal conduction in the absence of a magnetic field.

We can now read off  $\chi_0$  in (16). In a translationally invariant system in the absence of a magnetic field, the momentum conductivity  $\theta(\omega, 0) = i(\epsilon + P)/\omega T$  where  $\epsilon$  is the energy density and  $P$  the pressure. This result can be seen from hydrodynamics [8] or from the Ward identity arguments in [9]. The fact that the imaginary part of the conductivity behaves like  $1/\omega$  implies that the real part will contain a  $\delta(\omega)$ , because with some suitable  $i\epsilon$  prescription  $1/\omega = P(1/\omega) - i\pi\delta(\omega)$ . This delta function is expected for the energy flow in a translationally invariant system, which has no way to dissipate momentum. From the fact that translation invariance implies  $G_{\mathcal{P}\mathcal{P}}^R(\omega, 0) = 0$ , it follows that

$$\chi_0 = \epsilon + P. \quad (17)$$

That  $\chi_0 = \lim_{\omega \rightarrow 0} G_{\mathcal{P}\mathcal{P}}^R(\omega, 0)$  remains finite as  $\bar{V} \rightarrow 0$  is consistent with the fact that the  $\omega \rightarrow 0$  and  $\bar{V} \rightarrow 0$  limits of  $G_{\mathcal{P}\mathcal{P}}^R(\omega, 0)$  do not commute<sup>1</sup>.

### The memory function method

Now we extract the timescale from  $G_{\mathcal{P}\mathcal{P}}^R(\omega, 0)$ . The memory function  $M(\omega)$  is defined by

$$M(\omega) \equiv \frac{\omega G_{\mathcal{P}\mathcal{P}}^R(\omega, 0)}{\chi_0 - G_{\mathcal{P}\mathcal{P}}^R(\omega, 0)}, \quad (18)$$

which can be formally inverted to yield

$$G_{\mathcal{P}\mathcal{P}}^R(\omega, 0) = \frac{\chi_0 M(\omega)}{\omega + M(\omega)}. \quad (19)$$

The reason for introducing this function is to reinterpret the small  $\omega$  limit of  $M(\omega)$  as an inverse scattering time  $i/\tau_{\text{imp}}$ . We comment on this interpretation below. At finite  $\omega$ , by translational invariance we expect  $G_{\mathcal{P}\mathcal{P}}^R(\omega, 0)$  to vanish in the absence of impurities. We also expect that the inverse scattering time goes to zero with no impurities. Thus, consistent with eq. (18), we take both  $M(\omega)$  and  $G_{\mathcal{P}\mathcal{P}}^R(\omega, 0)$  to scale as  $\bar{V}^2$ . These statements do not hold when there is a nonvanishing background magnetic field. For the moment we are setting  $B = 0$ . As we noted,  $\chi_0 = G_{\mathcal{P}\mathcal{P}}^R(0, 0)$  is independent of  $\bar{V}$  to leading order. Thus from eq. (18), and using equation (15), we find the approximate expression for  $M(\omega)$ :

$$M(\omega) \approx \frac{\omega G_{\mathcal{P}\mathcal{P}}^R(\omega, 0)}{\chi_0} = \frac{-(G_{\mathcal{F}\mathcal{F}}^R(\omega, 0) - G_{\mathcal{F}\mathcal{F}}^R(0, 0))}{\chi_0} / \omega. \quad (20)$$

The approximation is up to terms of  $\mathcal{O}(\bar{V}^3)$ . We would like to take the small  $\omega$  limit of this expression. Because  $\bar{V}$  is dimensionful, one should expect that in order to obtain the true  $\omega \rightarrow 0$  limit it will be necessary to resum higher order contributions in  $\bar{V}/\omega^{2-\Delta_\phi}$ . Indeed, we have already noted that the  $\omega \rightarrow 0$  and  $\bar{V} \rightarrow 0$  limits do not commute. Using (20) directly to compute the relaxation timescale, is often called the ‘memory function method’, see for instance refs. [24, 25]. It was shown in ref. [26] that this method generally does not give the correct answer for small frequencies  $\omega^{2-\Delta_\phi} < \bar{V}$ .

We can obtain reliable results in the case when the temperature is large compared to the strength of the scattering potential:  $\bar{V}^{1/(2-\Delta_\phi)} \ll T$ . Given this separation of scales, at low frequencies

<sup>1</sup>In the absence of an external electric field,  $\theta$  is related to the thermal conductivity  $\bar{\kappa}$  and thermoelectric coefficient  $\hat{\alpha}$  defined, for example, in ref. [9] via  $\theta = \bar{\kappa} + \hat{\alpha}\mu$ . Thus at vanishing chemical potential  $\mu$ , the thermal conductivity is  $\theta$ . With no chemical potential, then  $\chi_0 = sT$ , with  $s$  the entropy density, leading to  $\bar{\kappa} = is/\omega$ .

$\omega \ll T$ , the constraint  $\omega^{2-\Delta_\phi} > \bar{V}$ , for the validity of perturbation theory, should be replaced by the weaker constraint  $T^{2-\Delta_\phi} > \bar{V}$ . In the language of the renormalization group,  $\bar{V}$  is a relevant operator and we must choose a scale at which to evaluate it. At nonzero temperature and at frequencies  $\omega < T$ , we expect the temperature to act as a cut off in the renormalization flow for  $\bar{V}$ . In higher order corrections to the memory function  $M$ , the ratio  $\bar{V}/T^{2-\Delta_\phi}$  will appear in place of  $\bar{V}/\omega^{2-\Delta_\phi}$ . Thus at high temperatures, we are justified in treating the impurities perturbatively, including at very low frequencies.

Evaluated perturbatively, the expression for the memory function (20) has an overall factor of  $\bar{V}^2$ , and no other dependence on  $\bar{V}$ . Scaling therefore implies that the frequency dependence must be some function of  $\omega/T$ . Thus the hydrodynamic limit  $\omega \ll T$  is equivalent to taking  $\omega \rightarrow 0$  in (20). We can identify

$$\begin{aligned} \frac{i}{\tau_{\text{imp}}} &= \frac{1}{\chi_0} \lim_{\omega \rightarrow 0} \frac{-(G_{\mathcal{FF}}^R(\omega, 0) - G_{\mathcal{FF}}^R(0, 0))}{\omega} \\ &= -\frac{1}{\chi_0} \left. \frac{dG_{\mathcal{FF}}^R(\omega, 0)}{d\omega} \right|_{\omega=0}. \end{aligned} \quad (21)$$

Using the fact that  $\text{Re } G_{\mathcal{FF}}^R$  is an even function while  $\text{Im } G_{\mathcal{FF}}^R$  is an odd function of  $\omega$ , we find our main result of the section that

$$\boxed{\frac{1}{\tau_{\text{imp}}} = -\frac{1}{\chi_0} \lim_{\omega \rightarrow 0} \frac{\text{Im } G_{\mathcal{FF}}^R(\omega, 0)}{\omega}}. \quad (22)$$

Let us clarify the physical meaning of  $\tau_{\text{imp}}$ . Strictly, the momentum relaxation timescale is given by the imaginary part of the pole in  $G_{\mathcal{PP}}^R(\omega, 0)$  that is closest to the real axis. The identification of the zero frequency limit as the inverse relaxation timescale

$$\frac{i}{\tau_{\text{imp}}} = \lim_{\omega \rightarrow 0} M(\omega), \quad (23)$$

is valid so long as the putative pole at  $-i/\tau_{\text{imp}}$  is sufficiently close to the real axis, in the sense that

$$\left| M\left(\frac{-i}{\tau_{\text{imp}}}\right) - \frac{i}{\tau_{\text{imp}}} \right| \ll \frac{1}{\tau_{\text{imp}}}. \quad (24)$$

It is easy to check, for instance, that this will be true if  $G_{\mathcal{PP}}^R(\omega, 0)$  has several poles, but one is much closer to the real axis than the others. Given that  $1/\tau_{\text{imp}} \sim \bar{V}^2/T^{3-2\Delta_\phi} \ll T$  is parametrically small compared to the temperature scale, we expect that (24) holds. However, if the coefficient of  $\bar{V}^2$  in (12) becomes sufficiently large, then that expression is no longer reliable as a relaxation timescale.

We argued above that at high temperatures, potentially dangerous  $\bar{V}/\omega^{2-\Delta_\phi}$  corrections would be replaced by corrections in  $\bar{V}/T^{2-\Delta_\phi}$ . While  $\bar{V}/\omega^{2-\Delta_\phi}$  corrections would tend to add more poles close to the origin of the complex  $\omega$  plane,  $\bar{V}/T^{2-\Delta_\phi}$  corrections are suppressed.

### 3.2 Impurity plus an external magnetic field

There is great formal similarity between adding to the Lagrangian a random potential coupled to a scalar operator  $\int d^3x V(x)\mathcal{O}(x)$  and adding an external  $U(1)$  gauge field coupled to a global current  $-\int d^3x A_\mu(x)J^\mu(x)$ . This second case was considered in detail in ref. [9]. A constant magnetic field has  $F=dA=B dx \wedge dy$ . Any potential  $A$  for this field strength will formally break translation invariance, which is one way to see why  $G_{\mathcal{PP}}^R(\omega, 0)$  can be nonzero in the absence of impurities but in the presence of a background magnetic field.

From the Ward identity results in ref. [9], with  $\bar{V} = 0$  one has

$$\omega G_{\mathcal{P}\mathcal{P}}^R(\omega, 0) = B^2 (G_{\mathcal{J}\mathcal{J}}^R(\omega, 0) - G_{\mathcal{J}\mathcal{J}}^R(0, 0)) / \omega, \quad (25)$$

where  $\mathcal{J} = J^i n_i$  is the electric current. The  $\omega \rightarrow 0$  limit of the current-current Green's function needs to be taken with care, as the  $B \rightarrow 0$  and  $\omega \rightarrow 0$  limits do not commute.

At  $\bar{V} = 0$ ,  $G_{\mathcal{J}\mathcal{J}}^R(0, 0)$  vanishes for real  $n_i$ , but there is still a Hall conductivity [7, 9],

$$\lim_{\omega \rightarrow 0} \frac{G_{J^x J^y}^R(\omega, 0)}{\omega} = i\rho/B. \quad (26)$$

To see the Hall effect within our formalism, it is convenient to let the  $n_i$  be complex and think of  $G^R$  as an inner product. This method of complexifying the conductivities was found to be useful in [9]. In this paper we will do so for this section and appendix B only. Taking  $n_i = (1, -i)/\sqrt{2}$ , we find

$$2G_{\mathcal{J}\mathcal{J}}^R = G_{J^x J^x}^R - iG_{J^x J^y}^R + iG_{J^y J^x}^R + G_{J^y J^y}^R. \quad (27)$$

By rotational invariance, this expression simplifies to

$$G_{\mathcal{J}\mathcal{J}}^R = G_{J^x J^x}^R - iG_{J^x J^y}^R. \quad (28)$$

Combining eqs. (25) and (15) then to include both impurities and a magnetic field leads to

$$\omega^2 G_{\mathcal{P}\mathcal{P}}^R(\omega, 0) = - (G_{\mathcal{F}\mathcal{F}}^R(\omega, 0) - G_{\mathcal{F}\mathcal{F}}^R(0, 0)) + B^2 (G_{\mathcal{J}\mathcal{J}}^R(\omega, 0) - \omega\rho/B). \quad (29)$$

Like eq. (15), we believe this expression is exact when the right hand side is evaluated in a background with nontrivial  $B$  and  $\bar{V}$  and  $G_{\mathcal{J}\mathcal{O}}^R = 0$ . We have been loose in our derivation, but the result can be made rigorous through a Ward identity argument. The potential cross term proportional to  $G_{\mathcal{J}\mathcal{O}}^R$  will vanish anyway to leading order in  $\bar{V}$  after averaging over  $V$ . But in fact, we will see shortly that the Green's function  $G_{\mathcal{J}\mathcal{O}}^R = 0$  vanishes for the M2 brane theory at leading order in  $1/N$  before averaging.

We call poles hydrodynamic if they are close to the origin of the complex  $\omega$  plane compared to the scales  $T$  and  $\rho$ . In the previous section, in the absence of a  $B$  field, we argued that for small  $\bar{V}$  there was a hydrodynamic pole in  $G_{\mathcal{P}\mathcal{P}}^R$  at  $-i/\tau_{\text{imp}}$ . In ref. [9], we saw that in the presence of a small magnetic field but in the absence of impurities, there are a pair of hydrodynamic poles at

$$\pm \omega_c - i\gamma = \frac{B(\pm\rho - i\sigma B)}{\epsilon + P}, \quad (30)$$

both in  $G_{\mathcal{P}\mathcal{P}}^R$  and  $G_{\mathcal{J}\mathcal{J}}^R$ . These poles correspond to damped relativistic cyclotron motion<sup>2</sup>. Here  $\sigma$  is the electrical conductivity of the CFT.

Physically, if we have a small but nonzero  $\bar{V}$  or  $B$ , we expect the  $\omega \rightarrow 0$  response of the system to be well behaved. The poles in the Green's functions should interpolate continuously between the cases in which either  $\bar{V}$  or  $B$  vanish. Thus, contemplating (29), it is natural to expect that the hydrodynamic poles in the presence of both  $\bar{V}$  and  $B$  are

$$-i\tau_{\text{imp}}^{-1} - i\gamma \pm \omega_c. \quad (31)$$

This combination of  $\tau_{\text{imp}}$  and the cyclotron pole was also found in the hydrodynamic analysis of [8]. In eq. (31) we see that there are two sources for momentum relaxation; one is impurities and the

---

<sup>2</sup>Again, our time dependence is  $e^{-i\omega t}$ . Thus  $\gamma > 0$  and  $\tau_{\text{imp}} > 0$  lead to exponential damping at long times.



other can naïvely be thought of as due to collisions of positively and negatively charged excitations of the theory undergoing cyclotron motion in opposite directions. In appendix B, we demonstrate how the memory function method can be used to extract the correct poles from the hydrodynamic expressions for  $G_{\mathcal{PP}}$  and  $G_{\mathcal{JJ}}$ , and we also show that these hydrodynamic expressions satisfy the relation (29).

The impurity relaxation timescale  $\tau_{\text{imp}}$  appearing in eq. (31) is given by the same formula as before, eq. (22), but can now have a  $B$  dependence, provided  $B$  is kept small so that our expression for the cyclotron pole is reliable. In more detail, our hydrodynamic expression for  $\gamma$  is correct to order  $B^2$  but we expect it to receive unknown corrections at  $\mathcal{O}(\bar{V}^2)$ . This is because the  $\epsilon + P$  appearing in the definition of  $\gamma$  in (30) will have a  $\bar{V}^2$  dependence. Our expression (22) for  $1/\tau$  is correct to order  $\bar{V}^2$  and in principle we know its full  $B$  dependence. However, we expect the hydrodynamic approximation to fail at  $\mathcal{O}(B^3)$ . Thus,  $1/\tau$  should be trustworthy at order  $\mathcal{O}(B^2\bar{V}^2)$  but no higher. Problematically, we do not know the corresponding  $\mathcal{O}(B^2\bar{V}^2)$  correction to  $\gamma$ . This uncertainty turns out not to be important for many of our considerations. In particular, when studying the Nernst effect at  $\rho = 0$  we will find that there is no dependence on  $\gamma$ .

## 4 Impurity relaxation in the truncated M2 brane theory

We have shown that computing the impurity relaxation timescale boils down to the two point function of equation (12). In this section we will perform the calculation for a truncation of the M2 brane CFT, using an adaptation of the AdS/CFT dictionary for real time two point functions proposed in [27]. As noted in the introduction, the truncation of the M2 brane theory is not consistent, and we make a nonstandard choice of conformal dimension for one of the scalars.

The CFT at finite temperature with a nonzero charge density and background magnetic field is dual to a dyonic black hole in  $AdS_4$  [7]. Such a black hole is a solution to Einstein-Maxwell theory with a negative cosmological constant. To this gravitational theory we would like to add a neutral scalar field  $\phi$  dual to our relevant operator  $\mathcal{O}$ .

From the M2 brane point of view, this Einstein-Maxwell theory with a neutral scalar should be a sector of eleven dimensional supergravity compactified on an  $S^7$ . After the compactification, we are left with an  $\mathcal{N} = 8$  supersymmetric gravitational theory on a four dimensional spacetime with a negative cosmological constant and infinite towers of Kaluza-Klein states. The isometry group  $SO(8)$  of the  $S^7$  determines many features of the lower dimensional theory.

It is believed to be consistent to truncate this compactification to the lowest states in the Kaluza-Klein towers. This truncation is called  $\mathcal{N} = 8$  gauged supergravity. The bosonic content of the truncation is the four dimensional graviton, an  $SO(8)$  gauge field, and a scalar and pseudoscalar transforming under 35 dimensional representations of  $SO(8)$ . These fields and their superpartners are thought not to act as sources for the other excited modes in the Kaluza-Klein towers, and hence the truncation is called consistent.

There exists a further truncation of  $\mathcal{N} = 8$  gauged supergravity to an abelian sector [28]. Consider the Cartan subalgebra of  $so(8)$ . The group  $SO(8)$  acts naturally on  $\mathbb{R}^8$ , and we can think of the elements of the Cartan subalgebra as generators of rotations in the 12, 34, 56, and 78 planes of  $\mathbb{R}^8$ . The action for the abelian truncation involves only the four  $U(1)$  gauge fields corresponding to these four rotations and the three scalar and pseudoscalar fields neutral under these four  $U(1)$  gauge groups. The full action for this abelian truncation can be found for example in ref. [29].

To see which scalar fields remain neutral, it is useful to think of the 35 dimensional representation

of  $SO(8)$  as the set of symmetric traceless quadratic polynomials in the coordinates on  $\mathbb{R}^8$ ,  $x^i x^j$ . The  $U(1)$ 's generated by the Cartan subalgebra act as phase rotations on the complex combinations  $z_i = x^{2i-1} \pm i x^{2i}$  for  $i = 1, 2, 3, 4$ . Thus the neutral quadratic scalars must be  $|z_i|^2 - |z_{i+1}|^2$ . There are three independent such scalars. By allowing the dual operators  $\mathcal{O}$  to couple to the impurity potential, we are breaking the  $SO(8)$  symmetry of the M2 brane theory. However, the operators are neutral under the  $U(1)$  symmetry for which we have a background  $B$  field and charge density. Indeed, models for ‘real world’ electronic systems often involve neutral impurities (see for example [30]).

We will make a further truncation of this theory and consider only the gauge field corresponding to a simultaneous rotation in all four planes, along with the scalar and pseudoscalar pair corresponding to just one of these neutral elements of the 35 dimensional representation. As we consider scalar two-point functions, we will only need the action to quadratic order in the scalars:

$$S = -\frac{1}{2\kappa_4^2} \int d^4x \sqrt{-g} \left( R - \frac{1}{2} [(\partial_\mu \phi)(\partial^\mu \phi) + (\partial_\mu \chi)(\partial^\mu \chi)] + 2L^{-2} \left[ 3 + \frac{1}{2}(\phi^2 + \chi^2) \right] - L^2 \left[ 1 + \frac{1}{2}(\phi^2 - \chi^2) \right] F_{\mu\nu} F^{\mu\nu} + \frac{1}{2} L^2 \phi \chi \epsilon^{\mu\nu\rho\sigma} F_{\mu\nu} F_{\rho\sigma} \right). \quad (32)$$

Here  $\epsilon^{\mu\nu\rho\sigma}$  is the totally antisymmetric tensor with  $\epsilon^{0123} = 1/\sqrt{-g}$ , and  $L$  is a length scale which determines the  $AdS$  radius. The dyonic black hole is a solution to the equations of motion provided that  $\phi = \chi = 0$ . As we can see in (32), however, the fact that  $\epsilon^{\mu\nu\rho\sigma} F_{\mu\nu} F_{\rho\sigma}$  does not vanish for the dyonic background implies that fluctuations in  $\phi$  and  $\chi$  source each other. This mixing is why we keep the two scalar fields. We comment below on the physical implications of the doubling.

We note that in a charged background, our final truncation to the two scalars plus the diagonal Maxwell field is not consistent. We have neglected a quadratic coupling between the neutral scalar fields and fluctuations of a non-diagonal combination of the four  $U(1)$  gauge fields of the full M2 brane theory [29]. Specifically, we are throwing away the terms

$$S_G = -\frac{1}{2\kappa_4^2} \int d^4x \sqrt{-g} \left( -L^2 G_{\mu\nu} G^{\mu\nu} - 2L^2 \phi F_{\mu\nu} G^{\mu\nu} + L^2 \chi \epsilon^{\mu\nu\rho\sigma} F_{\mu\nu} G_{\rho\sigma} \right), \quad (33)$$

where  $G_{\mu\nu} = \delta F_{\mu\nu}^{(1)} + \delta F_{\mu\nu}^{(2)} - \delta F_{\mu\nu}^{(3)} - \delta F_{\mu\nu}^{(4)}$  is the field strength for a non-diagonal subgroup of  $U(1)^4$ . We will continue to ignore this extra field for two reasons. Firstly, it makes the fluctuation analysis much more complicated. Secondly, from our condensed matter point of view, we need only one gauge field to model electricity and magnetism, and it is not clear to what this other gauge field would correspond. In appendix C we give more details about this coupling.

The black hole has metric

$$\frac{1}{L^2} ds^2 = \frac{\alpha^2}{z^2} [-f(z) dt^2 + dx^2 + dy^2] + \frac{1}{z^2} \frac{dz^2}{f(z)}, \quad (34)$$

and carries both electric and magnetic charge

$$F = h\alpha^2 dx \wedge dy + q\alpha dz \wedge dt, \quad (35)$$

where  $q, h$  and  $\alpha$  are constants. The function

$$f(z) = 1 + (h^2 + q^2)z^4 - (1 + h^2 + q^2)z^3. \quad (36)$$

The Hawking temperature, dual magnetic field and charge density of this black hole are [7]

$$B = h\alpha^2, \quad \rho = -q\alpha^2\sigma_0, \quad T = \frac{\alpha(3 - h^2 - q^2)}{4\pi}. \quad (37)$$

Note that  $q^2 + h^2 \leq 3$ , whereas  $\rho$  and  $B$  are unbounded. We have expressed the charge density in terms of the conductivity of the dual CFT at  $\rho = B = 0$ ,

$$\sigma_0 = 2L^2/\kappa_4^2 = \sqrt{2}N^{3/2}/6\pi. \quad (38)$$

In this last equality, we re-expressed the dimensionless  $L^2/\kappa_4^2$  in terms of the number  $N$  of coincident M2 branes [14]. These relations can be inverted to give  $\alpha(T, \rho, B)$  as the solution of

$$3\alpha^4 - 4\pi T\alpha^3 = B^2 + \rho^2/\sigma_0^2. \quad (39)$$

We would now like to consider small fluctuations of the scalar fields  $\phi$  and  $\chi$  about this black hole background. It is useful to diagonalise the quadratic Lagrangian (32) first by defining

$$\psi_+ = \frac{h\phi + q\chi}{\sqrt{q^2 + h^2}} \quad \text{and} \quad \psi_- = \frac{q\phi - h\chi}{\sqrt{q^2 + h^2}}. \quad (40)$$

The two fields will be dual to two relevant operators  $\mathcal{O}_\pm$ . For our dyonic black hole background

$$L^4 F_{\mu\nu} F^{\mu\nu} = 2z^4(h^2 - q^2), \quad \frac{1}{2}L^4 \epsilon^{\mu\nu\rho\sigma} F_{\mu\nu} F_{\rho\sigma} = -4z^4 hq. \quad (41)$$

Substituting into the action (32) one obtains the following decoupled actions for the scalar fields

$$S_\pm = -\frac{1}{2\kappa_4^2} \int d^4x \sqrt{-g} \left( -\frac{1}{2} (\partial_\mu \psi_\pm) (\partial^\mu \psi_\pm) + \frac{1}{L^2} [1 \mp z^4(q^2 + h^2)] \psi_\pm^2 \right). \quad (42)$$

The equations of motion are therefore

$$\square \psi_\pm = (m^2 \pm 2z^4(q^2 + h^2)/L^2) \psi_\pm, \quad (43)$$

where  $m^2 L^2 = -2$ . Note that this mass is above the Breitenlohner-Freedman bound  $m^2 L^2 \geq -9/4$ . Depending on the sign of  $\pm$ , the electromagnetic field provides a potential for the scalar that either pushes the scalar away from or towards the horizon. We will assume that the scalar field has the following dependence on  $x$ ,  $y$ , and  $t$ :  $\phi \sim e^{ikx - i\omega t}$ . Thus, the equation of motion becomes

$$z^4 \left( \frac{f}{z^2} \psi'_\pm \right)' - \mathfrak{q}^2 z^2 \psi_\pm + \mathfrak{w}^2 \frac{z^2}{f} \psi_\pm - m^2 L^2 \psi_\pm \mp 2z^4(q^2 + h^2) \psi_\pm = 0, \quad (44)$$

where we have defined the dimensionless frequency and wavevector  $\mathfrak{w} \equiv \omega/\alpha$  and  $\mathfrak{q} \equiv k/\alpha$ , and also  $f' = df/dz$ . Near the boundary,  $z = 0$ , of this asymptotically  $AdS_4$  geometry, the scalar has the usual behavior

$$\psi_\pm = z^{3-\Delta} (A(\omega, k) + \mathcal{O}(z^2)) + z^\Delta (B(\omega, k) + \mathcal{O}(z^2)), \quad (45)$$

where  $\Delta(\Delta - 3) = m^2 L^2$ .

In the standard M2 brane theory, representation theory of  $SO(8)$  and the superconformal symmetry guarantees that  $\phi$  has conformal dimension  $\Delta_\phi = 1$  while the pseudoscalar  $\chi$  has dimension  $\Delta_\chi = 2$  [14, 21, 22, 23]. Introducing nonzero  $B$  and  $\rho$ , as we have seen, mixes  $\phi$  and  $\chi$ . We speculate that in the dyonic black hole background, it is the linear combinations  $\psi_\pm$  which have definite conformal dimension rather than  $\phi$  and  $\chi$  independently. We shall avoid these subtleties by taking both  $\phi$  and  $\chi$  to have dimension  $\Delta_\phi = 1$ . The standard M2 brane theory is related to this choice of conformal dimension by a deformation by a double trace operator [13]. This choice has the added benefit of providing a second scalar to analyze with conformal dimension one, and therefore relevant.

The dimensions  $\Delta_\phi = 1$  and  $\Delta_\chi = 2$  both correspond to the mass  $m^2 L^2 = -2$ . The fact that there are two possible conformal dimensions associated with the same mass has important

consequences here. Having chosen the smaller conformal dimension, it is the faster falloff that is dual to a source for  $\mathcal{O}$  in the boundary theory [31]

$$J_{\mathcal{O}} = \alpha^{3-\Delta_{\mathcal{O}}} A(\omega, k), \quad (46)$$

whereas the slower falloff gives the expectation value

$$\langle \mathcal{O} \rangle = \frac{\sigma_0}{4} \alpha^{\Delta_{\mathcal{O}}} (2\Delta_{\mathcal{O}} - 3) B(\omega, k). \quad (47)$$

From these expressions one can read off the Green's function

$$\langle \mathcal{O} \rangle = G_{\mathcal{O}\mathcal{O}}^R(\omega, k) J_{\mathcal{O}}. \quad (48)$$

Thus

$$G_{\mathcal{O}\mathcal{O}}^R(\omega, k) = -\frac{\sigma_0}{4\alpha} \frac{B(\omega, k)}{A(\omega, k)}. \quad (49)$$

The standard procedure for scalars of mass  $m^2 L^2 = -2$  would have yielded  $G_{\mathcal{O}\mathcal{O}}^R \sim A/B$ . Because our operators have the smaller conformal dimension, we get the result (49).

Our job is to determine the dimensionless function  $F$  appearing in the scaling relation (13). We will need to compute two scaling functions  $F_{\pm}$ , one for each scalar field  $\psi_{\pm}$ . An observation that simplifies our task is that the differential equation (44) depends on  $B$  and  $\rho$  only in the combination  $h^2 + q^2$ , or equivalently  $B^2 + \rho^2/\sigma_0^2$ . Thus,  $F$  is a function of  $B^2 + \rho^2/\sigma_0^2$  only<sup>3</sup>. Using the fact that for the dyonic black hole [7, 9]

$$\epsilon = \frac{\sigma_0 \alpha^3}{2} (1 + h^2 + q^2), \quad P = \frac{\epsilon}{2}, \quad s = \pi \sigma_0 \alpha^2, \quad (50)$$

and that for the M2 theory (12) becomes

$$\boxed{\frac{1}{\tau_{\text{imp}}} = \frac{\bar{V}^2}{T} F\left(\frac{1}{T^2} \sqrt{B^2 + \rho^2/\sigma_0^2}\right)}, \quad (51)$$

the expressions in the preceding paragraphs imply that

$$\boxed{F\left(\frac{1}{T^2} \sqrt{B^2 + \rho^2/\sigma_0^2}\right) = -\frac{sT}{16\pi^2(\epsilon + P)} \lim_{\mathfrak{w} \rightarrow 0} \int d\mathfrak{q} \, \mathfrak{q}^3 \text{Im} \frac{B(\mathfrak{w}, \mathfrak{q})}{\mathfrak{w} A(\mathfrak{w}, \mathfrak{q})}}. \quad (52)$$

It is interesting to recall from [9] that the dc conductivity for the M2 brane, with nonvanishing  $B$  and  $\rho$  is given by

$$\sigma = \frac{(sT)^2}{(\epsilon + P)^2} \sigma_0, \quad (53)$$

allowing us to rewrite (52) as

$$F\left(\frac{1}{T^2} \sqrt{B^2 + \rho^2/\sigma_0^2}\right) = -\frac{1}{16\pi^2} \sqrt{\frac{\sigma}{\sigma_0}} \lim_{\mathfrak{w} \rightarrow 0} \int d\mathfrak{q} \, \mathfrak{q}^3 \text{Im} \frac{B(\mathfrak{w}, \mathfrak{q})}{\mathfrak{w} A(\mathfrak{w}, \mathfrak{q})}. \quad (54)$$

The physical meaning of this formula is not clear, because in general there's no particular reason for the impurity relaxation timescale to be related to the electrical conductivity of the CFT in the absence of impurities. It remains for us to solve for  $A(\mathfrak{w}, \mathfrak{q})$  and  $B(\mathfrak{w}, \mathfrak{q})$  numerically.

<sup>3</sup>Amusingly, this dependence only on the combination  $h^2 + q^2$  remains true in the full M2 brane theory, in which one keeps the second gauge field to which  $\phi$  and  $\chi$  couple. See appendix C.

## 4.1 Comment on discrete symmetries

Before turning to computations, we should comment that we have found two relevant operators  $\mathcal{O}_\pm$ , both with dimension  $\Delta_{\mathcal{O}_\pm} = 1$ . Both operators preserve the global  $U(1)$  symmetry and in principle, they could both be sourced by impurities. However, these operators transform differently under the discrete symmetries charge conjugation  $\mathcal{C}$ , parity  $\mathcal{P}$ , and time reversal  $\mathcal{T}$ .

Usually we make a sharp distinction between the way operators transform and the way states transform. The situation here is complicated by the fact that our fields  $\psi_\pm$  dual to the  $\mathcal{O}_\pm$ , and hence the  $\mathcal{O}_\pm$  themselves, are defined in (40) in terms of the state and in particular the choice of background magnetic field  $B$  and charge density  $\rho$ . In studying  $\psi_\pm$ , when we act with  $\mathcal{C}$ ,  $\mathcal{P}$ , and  $\mathcal{T}$ , we will act on both the operator and the underlying state.

From the gauged  $\mathcal{N} = 8$  supergravity construction we know that  $\phi$  and  $\chi$  are both real fields and thus do not transform under  $\mathcal{C}$ . At the same time  $\phi$  is a scalar while  $\chi$  is a pseudoscalar. Thus we have  $\mathcal{P}(\phi) = \phi$  and  $\mathcal{P}(\chi) = -\chi$ . From the CPT theorem, we must have under time reversal that  $\mathcal{T}(\phi) = \phi$  while  $\mathcal{T}(\chi) = -\chi$ .

The transformation properties of the electromagnetic field under  $\mathcal{C}$ ,  $\mathcal{P}$ , and  $\mathcal{T}$  are well known. In our case, the strength of the electric field of the black hole, which is dual to the charge density  $\rho$  on the boundary, is characterized by the value of  $q$ . The magnetic field strength  $B$  is fixed by the value of  $h$ . Under parity, we know the electric field is a vector while the magnetic field is a pseudovector. Thus we have  $\mathcal{P}(q) = -q$  while  $\mathcal{P}(h) = h$ .  $\mathcal{C}$  flips the sign of both  $q$  and  $h$ . Finally, the magnetic field famously breaks time reversal symmetry, and so  $\mathcal{T}(h) = -h$  while  $\mathcal{T}(q) = q$ .

Assembling these facts about  $q$ ,  $h$ ,  $\phi$  and  $\chi$  together we find that

$$\begin{aligned} \mathcal{C}(\psi_+) &= -\psi_+ , & \mathcal{P}(\psi_+) &= \psi_+ , & \mathcal{T}(\psi_+) &= -\psi_+ , \\ \mathcal{C}(\psi_-) &= -\psi_- , & \mathcal{P}(\psi_-) &= -\psi_- , & \mathcal{T}(\psi_-) &= \psi_- . \end{aligned} \tag{55}$$

The subscript of  $\psi_\pm$  thus corresponds to the eigenvalue of the field under  $\mathcal{P}$ . In adding impurities, we are faced with a choice: we can let the impurities break  $\mathcal{T}$  but not  $\mathcal{P}$  or  $\mathcal{P}$  but not  $\mathcal{T}$ . In the next section, we will see the behavior of the scattering time  $\tau_{\text{imp}}$  for the  $\mathcal{O}_+$  impurities is markedly different from the  $\mathcal{O}_-$  impurities.

Note that  $\mathcal{O}_+$  transforms the same way under the discrete symmetries as the magnetic field while  $\mathcal{O}_-$  transforms as the electric field. It is thus tempting to call the  $\mathcal{O}_+$  impurities magnetic and the  $\mathcal{O}_-$  impurities electric. The underlying scalar fields  $\phi$  and  $\chi$  are of course neutral. The nontrivial transformation of  $\psi_\pm$  under  $\mathcal{C}$  comes from the dressing by the dyonic black hole background, or equivalently, the presence of magnetic field and charge density in the field theory.

## 5 Numerical results for $1/\tau_{\text{imp}}$

The prescription for computing the retarded Green's function [27] is that we solve the equation for our scalar field in the black hole background (44) with ingoing boundary conditions at the black hole horizon  $z = 1$ ,

$$\psi \sim (1 - z)^{i\omega/(h^2 + q^2 - 3)} . \tag{56}$$

It is convenient to impose these boundary conditions by defining a new function  $S(z)$  such that

$$\psi(z) \equiv \exp \left( i\omega \int_0^z \frac{x^2}{f(x)} dx \right) S(z) . \tag{57}$$

Thus  $S(z)$  is nicely behaved at the horizon and we can impose  $S(1) = 1$ . It is straightforward to integrate the equation for  $S(z)$  numerically from the horizon to the boundary at  $z = 0$ . Near the boundary one can read off the value of the ratio  $B/A$  that we need to compute the scaling function  $F$ .

Given  $B/A$ , we then need to compute the integral (52) over  $k$ . This integral may not converge, and indeed we discuss below a large  $\rho$  and  $B$  regime where it does not for the  $\psi_-$  scalar field. However, the divergence comes from bad behavior at finite  $k$ . At large  $k$  we expect the imaginary part of the Green's function to be exponentially damped. Appendix D presents a WKB analysis that demonstrates this damping. Qualitatively, we may understand the behavior from the bulk as follows. At large  $k$ , the Green's function is dominated by a space-like geodesic which stays close to the boundary of the space-time and far from the black hole horizon; it is the horizon that is responsible for producing dissipative effects and a nonzero contribution to the imaginary part of the Green's function.

We begin by considering the two point function corresponding to the scalar field  $\psi_+$ , that is, magnetic impurities. The result for  $F_+$  is plotted in figure 1a. As the combination  $B^2 + \rho^2/\sigma_0^2$  is increased, the inverse scattering time becomes smaller and smaller. There is also a competing physical process that we described in section 3.2 above: the cyclotron resonance. If we keep  $B/T^2$  small ( $h \ll 1$ ), then we can trust our hydrodynamic approximation of the location of the cyclotron pole at  $\omega_c - i\gamma$ , given in (30). In figure 2, we plot the dimensionless  $\gamma/T$  against  $\rho/T^2\sigma_0$  for an appropriately small  $B/T^2 = 1$ . We see that at large  $\rho$ , the damping due to the cyclotron resonance also gets small while the frequency changes more slowly. The reduction in damping both from impurities and the  $B$  field at large  $\rho$  may make the hydrodynamic cyclotron mode easier to observe experimentally than the results in [8] suggested, as there the dependence of  $\tau_{\text{imp}}$  on  $B$  and  $\rho$  was not considered.

We also would like to consider the scaling function  $F_-$  for the  $\psi_-$  scalar fields. The result is plotted in figure 1b, and is somewhat dramatic. We define the related dimensionless quantities

$$Q \equiv \sqrt{h^2 + q^2} \quad \text{and} \quad \mathcal{Q} \equiv \frac{1}{T^2} \sqrt{B^2 + \rho^2/\sigma_0^2}. \quad (58)$$

We find that  $F_-$  increases monotonically as a function of  $Q$  or  $\mathcal{Q}$  and at a finite value  $Q_* = 0.76654$ , which corresponds to  $\mathcal{Q}_* = 20.80$ ,  $1/\tau_{\text{imp}}$  diverges. This divergence reveals some interesting physics in the 'pure' CFT which we will return to shortly. Note that we cannot trust our memory function formalism if  $1/\tau_{\text{imp}}$  gets too large. Higher order and nonperturbative effects are important in this regime.

From a gravitational standpoint, we may attempt a qualitative understanding of the decrease (increase) of  $1/\tau_{\text{imp}}$  with  $\rho$  and  $B$  for the  $\psi_+$  ( $\psi_-$ ) field. From (44), the scalar  $\psi_{\pm}$  experiences a potential of the form  $\pm 2z^4(h^2 + q^2)$ . Thus for  $\psi_+$ , the potential repels the scalar from the black hole horizon while for  $\psi_-$ , the potential has the opposite effect. The black hole horizon is responsible for dissipation in the system, and we expect the more the probability distribution of the scalar is peaked near the horizon, the larger the imaginary part of the scalar Green's function will be and hence the larger  $1/\tau_{\text{imp}}$  will be. The decrease in  $F_{\pm}$  with  $B$  and  $\rho$  for  $\psi_+$  and the corresponding increase for  $\psi_-$  in figures 1a and 1b are thus qualitatively understood.

## 5.1 A black hole instability

The divergence in  $F_-$  is caused by an underlying instability in the truncated M2 brane theory at large  $\mathcal{Q}$ . Numerically we have found that the divergence in  $F_-$  appears to be caused by a diffusion

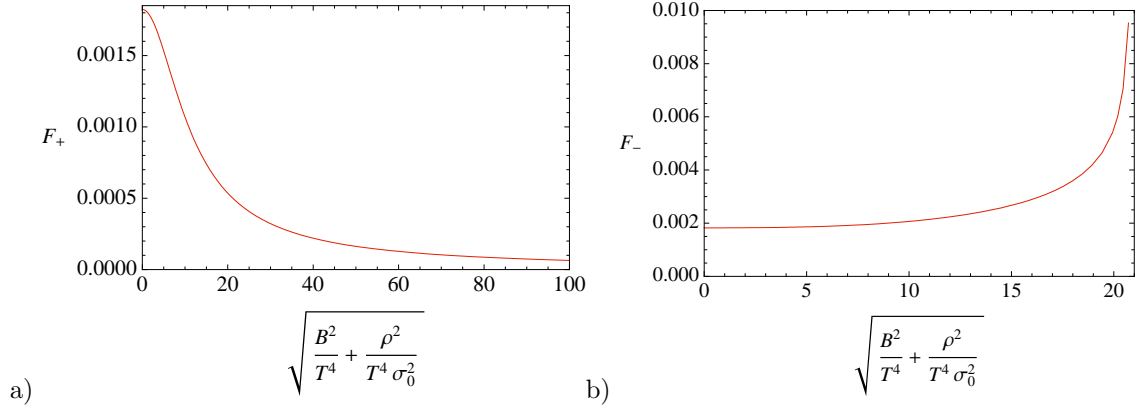


Figure 1: The function  $F_{\pm}$  for the M2 brane theory for a) the scalar field  $\psi_+$  and b)  $\psi_-$ .

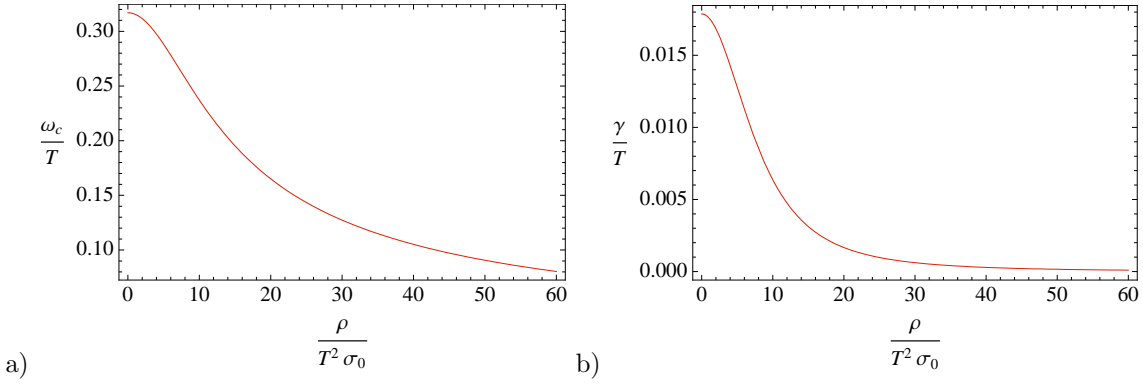


Figure 2: a) The real part of the cyclotron frequency and b) momentum relaxation due to the cyclotron resonance at  $B = T^2$ .

type pole in the scalar Green's function moving onto the real  $k$  axis. Near the critical value  $Q_*$ , the pole has the approximate form

$$G_{\mathcal{O}\mathcal{O}}^R \sim \frac{1}{C(h, q) - q^2 + 6i\mathfrak{w}/5 + \dots} . \quad (59)$$

The ellipsis denotes higher order terms in  $\omega$  and  $k$  and  $C(h, q) = 1.3911(Q - Q_*)$ . In figures 3a and b we have plotted the location of the pole as a function of  $Q$ . Note that in both plots, for  $k^2$  and  $\text{Im}\omega$ , the curves reach the real axis at  $Q_* = 20.80$ . At this point, two changes occur simultaneously. First,  $1/\tau_{\text{imp}}$  diverges because, at  $\omega = 0$ , there is a (double) pole on the real  $k$  axis that is integrated over in (52). Second, at  $k = 0$ , the imaginary part of  $\omega$  switches sign leading to exponential growth in the scalar mode at long times.

This exponential growth in time is indicative of an underlying instability in the CFT when  $Q > Q_*$ . Indeed, the retarded Green's function cannot have poles in the upper half  $\omega$  plane, indicating that for  $Q > Q_*$  we are no longer in the correct vacuum. To evaluate the impurity time for  $Q > Q_*$ , we would need to find a different stable supergravity background in which the  $\psi_-$  field was at a local minimum. This instability illustrates the dangers in this particular black hole background of working in a consistent truncation in which we set  $\psi_- = 0$ ; had we ignored fluctuations in  $\psi_-$ , we would have missed this instability.

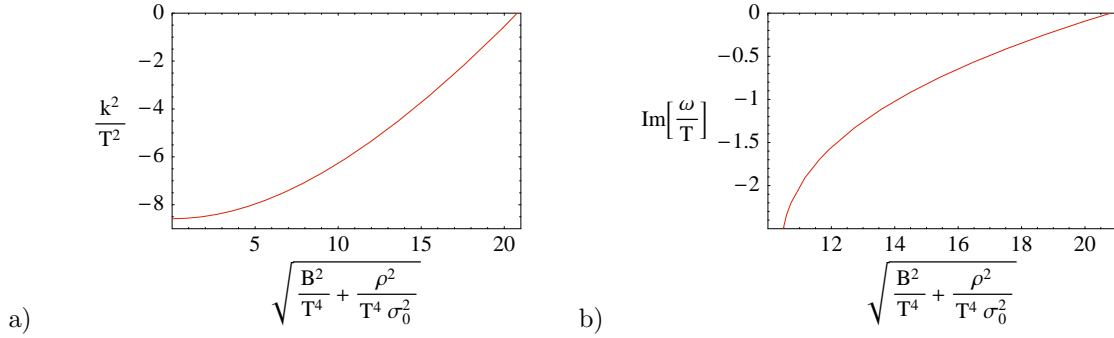


Figure 3: The location of the smallest pole in  $G_{\mathcal{O}_-\mathcal{O}_-}^R$  as a function of  $B$  and  $\rho$ : a) The pole in the complex  $k$  plane for  $\omega = 0$ . Note  $k^2$  is real. b) The pole in the complex  $\omega$  plane for  $k = 0$ . Note  $\text{Re}(\omega) = 0$ .

This instability in the theory is interesting from a purely gravitational perspective. First note that poles in the Green's function (49) occur when the denominator  $A(\omega, k)$  vanishes. This vanishing means there exist on shell modes with the behaviour  $\psi_{\pm} = z + \mathcal{O}(z^3)$  near the conformal boundary  $z = 0$ . Due to the nonstandard boundary conditions for the  $\psi_{\pm}$  fields, these modes are physical. For the critical value  $Q = Q_*$ , the physical mode is static, with  $\omega = 0$ . This ‘threshold’ mode separates oscillating modes, with  $Q < Q_*$  and  $\text{Im } \omega < 0$ , from exponentially growing modes, with  $Q > Q_*$  and  $\text{Im } \omega > 0$ . For  $Q > Q_*$  there is an on shell classical instability of the black hole.

A classical instability of the full finite temperature M2 brane was discovered in [15, 16]. To see that instability, it is necessary to retain more than one Maxwell field in the bulk, whereas we have truncated to a diagonal combination. Converting to our variables, the Gubser-Mitra instability occurs with  $h = 0$  and at  $q_{GM} = 1$ , corresponding to the value  $\rho_{GM}/\sigma_0 T^2 \approx 39.5$ . This charge density is larger than necessary for the instability we have described. Given that the two instabilities occur in different theories, one might be cautious about attaching much meaning to the relative values of the critical charges<sup>4</sup>.

The classical Gubser-Mitra instability occurs at precisely the same value of the charge density at which the charged black hole with four  $U(1)$  gauge fields becomes thermodynamically unstable. This coincidence led Gubser and Mitra to the ‘correlated stability’ conjecture, that for translationally invariant horizons, thermodynamic and classical dynamic instabilities should always coincide.

In contrast, our black hole with only one  $U(1)$  gauge field is always thermodynamically stable [7]; it only becomes thermodynamically unstable when embedded into the full M2 brane theory, with four independent charges. Given this dynamical instability without a corresponding thermodynamic instability, we have a counterexample to the correlated stability conjecture. The physics underlying our counterexample appears to be very similar to the counterexamples discussed in [17]. The mismatch between thermodynamic and classical instability is possible because the instability is due to scalar fields that are not associated to conserved charges. The instability indicates a phase transition to an ordered phase, characterised by a condensate for the operator  $\mathcal{O}_-$  dual to the field

<sup>4</sup>In fact, the analysis in [15, 16] also employs an inconsistent truncation. Although that work does include the gauge field  $G$ , it does not include the pseudoscalar  $\chi$ , which is sourced by  $G$ . See appendix C. For an investigation of threshold modes  $\omega = k = 0$ , this  $\chi G_{xy}$  coupling will vanish and so should not affect the location of the Gubser-Mitra instability. Note also, [15, 16] work with conformal dimension  $\Delta = 2$  for the operator dual to  $\phi$ , so their dual theory is also related to the standard M2 brane theory by a double trace deformation.



$\psi_-$ . As noted in [17], it seems appropriate to widen the notion of thermodynamic instability of black holes in these cases to allow for variations of the value of the scalar field at the conformal boundary. Because this phase transition is associated with breaking an underlying  $\mathbb{Z}_2$  symmetry,  $\psi_- \rightarrow -\psi_-$ , of the truncated supergravity action, the transition is likely to be second order.

## 6 The Nernst effect in the truncated M2 brane theory

Place a system in a thermal gradient and a perpendicular magnetic field. The Nernst effect is the observation of an electric field that is created orthogonal to both the thermal gradient and the background magnetic field. The Nernst coefficient is the electric field generated per unit of thermal gradient and magnetic field

$$N = \frac{E}{B\nabla T}. \quad (60)$$

Recent experimental interest in the Nernst effect in superconductors was sparked by the observation by Ong et al. of an anomalously large Nernst effect in the pseudogap region of the high- $T_c$  superconductors [32]. This observation was interpreted as signalling the presence of vortices, and hence the persistence of a phase disordered Cooper pair condensate, above the transition temperature. The Nernst effect has since been used to probe the presence of long lived Cooper pair fluctuations in conventional superconductors [33] and also to capture the proximity of a Mott insulating phase in certain organic superconductors [18].

The Nernst effect depends strongly on the impurity relaxation time. Therefore, the  $B$  and  $\rho$  dependence of  $\tau_{\text{imp}}$  that we explored above may have measurable consequences for observations of the Nernst effect in various types of superconductors. In this section, we explore the dependence of the Nernst effect on  $\tau_{\text{imp}}$ . We argue that there are qualitative similarities between aspects of the  $T$  and  $B$  dependence of the Nernst effect observed in organic superconductors [18] and the Nernst effect we predict at  $\rho = 0$ . In the underdoped cuprate superconductors [32, 34], for a range of typical values of the doping, we find that the relatively large size of  $\rho$  compared with experimentally accessible values of  $B$  make  $\tau_{\text{imp}}$  relatively insensitive to  $B$ . The exception to this last statement is very close to the insulating state at doping  $x_I = 1/8$ , where  $\rho = 0$  is again appropriate.

A hydrodynamic approach to the Nernst effect was developed in ref. [8]. That work led to the following formula for the Nernst coefficient in a relativistic theory with ‘speed of light’  $v$ . For the next couple of formulae only we shall not set  $v = 1$ , as we have been doing in this paper, and shall also show explicitly the unit electric charge  $e$ . It was found that

$$N = \frac{v^2}{T} \left( \frac{1/\tau_{\text{imp}}}{(\omega_c^2/\gamma + 1/\tau_{\text{imp}})^2 + \omega_c^2} \right). \quad (61)$$

Restoring the  $v$  and  $e$  dependence of the cyclotron pole, we have

$$\omega_c = \frac{eB\rho v^2}{\epsilon + P} \quad \text{and} \quad \gamma = \frac{\sigma B^2 v^2}{\epsilon + P}. \quad (62)$$

In ref. [8] the hydrodynamic expression (61) was used to reproduce some features of the experimentally observed Nernst effect in the cuprates. However, in the absence of a microscopic theory, the simplifying assumption was made that the functions of state, the conductivity  $\sigma$  and the impurity scattering time  $\tau_{\text{imp}}$  did not depend significantly on the dimensionless ratios  $\rho/T^2$  and  $B/T^2$ . For the M2 brane theory,  $\sigma(\rho/T^2, B/T^2)$  was computed in ref. [9], and in this paper we have computed  $\tau_{\text{imp}}$ . Thus we have all the ingredients necessary for an exact computation of the Nernst coefficient at a quantum critical point.

The Nernst effect is a direct probe of the impurity relaxation time. We see in (61) that a nonzero  $\tau_{\text{imp}}$  is necessary for the Nernst coefficient to be finite. This connection becomes particularly striking in the limit of vanishing charge density,  $\rho = 0$ , where (61) becomes simply

$$N = \frac{v^2 \tau_{\text{imp}}}{T} = \frac{v^2}{\bar{V}^2 F(B/T^2)}, \quad (63)$$

where in the second step we used (51) for the M2 brane theory. One nice feature of this formula is that the dependence on  $\gamma$  has dropped out, and with it the uncertainties of order  $\bar{V}^2 B^2$  that we discussed at the end of section 3.2.

Using our numerical results from the previous section, it is straightforward to plot the Nernst coefficient for the truncated M2 brane theory as a function of  $B$  and  $T$ , which is how the experimental data is often presented [18, 34, 35]. In figure 4a we plot the Nernst coefficient in the case of vanishing charge density (63). We have taken the impurity potential to couple to the  $\mathcal{O}_+$  operator. If we had taken the  $\mathcal{O}_-$  operator, the dark and light regions of the plot would have been interchanged. For ease of comparison with experiments, we should consider plotting in SI units. In order to convert  $B/T^2$  from our ‘natural units’, with  $v = k_B = \hbar = e = 1$ , one must first introduce the velocity  $v = \Phi_v \text{m/s}$ , and then note that

$$\frac{\text{tesla}}{(\text{kelvin})^2} = 8.8 \times 10^{-8} \Phi_v^2 \frac{k_B^2}{e \hbar v^2}. \quad (64)$$

We now need to specify the number  $\Phi_v$ . A convenient choice is  $\Phi_v = 3400$ , as this makes the conversion factor  $8.8 \times 10^{-8} \Phi_v^2 = 1$ . Curiously, this appears to be in a physically reasonable ballpark, at least for the cuprate superconductors. This value corresponds to  $\hbar v = 22 \text{ meV } \text{\AA}$ , whereas the value estimated in [8] for underdoped LSCO was  $47 \text{ meV } \text{\AA}$  and the characteristic velocity observed in YBCO was  $35 \text{ meV } \text{\AA}$  [36]. While all plots in this section are in natural units, in figure 4a, for concreteness only, we have assumed  $\hbar v = 22 \text{ meV } \text{\AA}$  and put kelvin and tesla on the axis labels.

In figure 4a, the range of temperatures and magnetic fields has been constrained by the validity of the hydrodynamic approximation, which for the M2 brane theory requires  $B/T^2 \lesssim 10$  [9]. Outside this regime one does not expect (61) to hold. Although the M2 brane theory can be studied beyond the hydrodynamic regime [9], in that case our arguments in section 3.2 for combining the effect of impurities and the magnetic field do not hold.

The qualitative form of figure 4a is determined from the fact that  $N \sim 1/F(B/T^2)$ , with  $F$  a monotonically decreasing function. This scaling will be a universal feature of the Nernst effect at  $\rho = 0$  in the vicinity of a quantum critical point. The scaling near a general quantum critical point will be

$$N \sim \frac{T^{2-2\Delta_{\mathcal{O}}}}{F(B/T^2)}. \quad (65)$$

We illustrate this general form in figure 4b, taking  $F(x) = 1/(1+x^2)$  for concreteness. It is interesting to note that this qualitative form appears to arise in Fig. 3b of ref. [18] at low magnetic fields and just above the superconducting phase transition temperature,  $T_c$ . The authors of ref. [18] study organic superconductors, and their Fig. 3b is, like our figure 4, a plot of  $N(T, B)$ . Their system also has zero charge density, as it is not doped. The region of interest (low  $B$ , just above  $T_c$ ) is precisely that for which [18] propose that strongly correlated electron physics is important, as are the effects of a nearby Mott transition.

We can try to compute the Nernst signal with a finite charge density using the formula (61). As a benchmark, one can compare with experimental results for the underdoped cuprate superconductors.

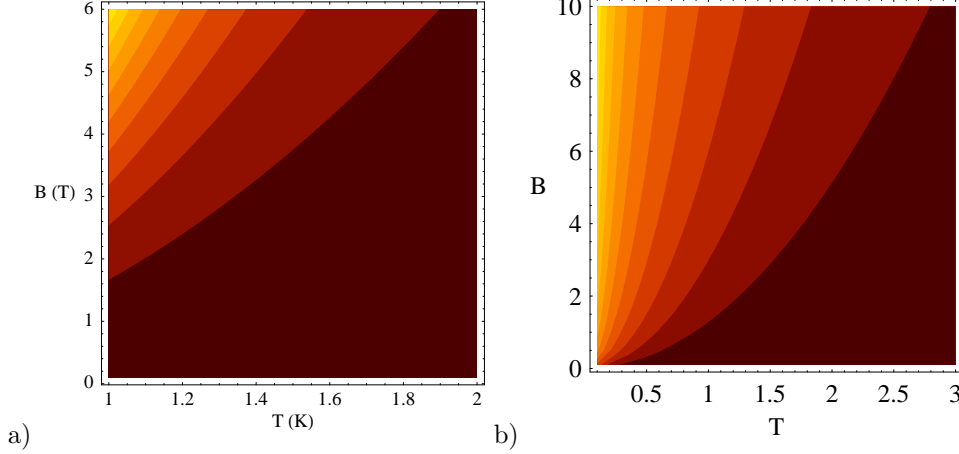


Figure 4: (a) The Nernst signal  $N$  for the truncated M2 brane theory as a function of  $B$  and  $T$ , with vanishing charge density  $\rho = 0$ . The impurity potential is coupled to  $\mathcal{O}_+$ . Lighter denotes a larger Nernst coefficient. (b) The Nernst signal in the vicinity of a general quantum critical point with  $\rho = 0$  and  $\Delta_{\mathcal{O}} = 1$ . The shading is logarithmically spaced.

It was argued in [8] that the charge density was given by the difference in the doping from the commensurate insulating state at  $x_I = 1/8$ , divided by the area of a unit lattice cell. For underdoped LSCO, at  $x - x_I = -0.025$  for example, the lattice constant is  $a = 3.78 \text{ \AA}$ , leading to

$$\rho = \frac{e(x - x_I)}{a^2} \approx 0.028 \frac{\text{C}}{\text{m}^2}. \quad (66)$$

The conductivity at the critical point can be estimated to be [37]

$$\sigma_0 \approx \frac{4e^2}{h} \approx 1.6 \times 10^{-4} \frac{\text{C}^2}{\text{J s}}, \quad (67)$$

allowing us to obtain

$$\frac{\rho}{\sigma_0} \approx 175 \text{ tesla}. \quad (68)$$

We have expressed the result in tesla, so that it may be compared to the value of the background magnetic field. The value of 175 tesla is significantly larger than the typical magnetic fields applied in experiments measuring the Nernst effect in the cuprate superconductors. In our expression for the Nernst coefficient, the magnetic field  $B$  only appears in the combination  $B^2 + \rho^2/\sigma_0^2$ . Therefore the large value of the charge density in (68) swamps out the  $B$  dependence, and the resulting plot of  $N(T, B)$  shows simply vertical lines. We might note however that both (66) and (67) are only tentative identifications, so the result (68) could change substantially. In particular, the conductivity (67) assumes the putative nearby superconductor-insulator quantum phase transition in the cuprates is in the same universality class as the films reviewed in [37].

It was suggested in [8] that the quantity that should be compared with measurements of the Nernst effect in the cuprates is not  $N$ , but rather the off diagonal thermoelectric coefficient  $\alpha_{xy}$ . This was to isolate the contribution of critical superconducting fluctuations from non-critical fermionic contributions to the conductivity. This coefficient gives the electrical current generated by an applied thermal gradient:  $J_x = -\alpha_{xy} \partial_y T$ . It is related to the Nernst response by the electrical conductivity, roughly  $\alpha_{xy} \approx \sigma_{xx} B N$ . Here  $\sigma_{xx}$  is the full conductivity of the system, not just that of the critical

fluctuations. The thermoelectric coefficient has a  $B$  dependence that is not swamped out by a large charge density [8], and indeed reproduces various features of the experimental data for  $N(T, B)$  in the cuprates. The large charge density implies that if we use our M2 brane expressions for the impurity timescale  $\tau_{\text{imp}}(\rho, B, T)$ , we will not introduce any extra dependence on  $B$  into the previous results of [8]. In any case, the high critical temperature of the cuprates combined with the value for the velocity  $v$ , discussed above, implies that  $B/T^2, \rho/T^2 \ll 1$  over the region of interest. Therefore it is consistent to neglect the  $B$  and  $\rho$  dependence of  $\tau_{\text{imp}}$  and the  $\epsilon + P$  for these systems.

In figure 5 we have plotted the Nernst coefficient for the truncated M2 brane theory with  $\rho/\sigma_0 = 8.3 \times 10^{-5}$  and  $\rho/\sigma_0 = 10$ , in each case with  $\bar{V} = 0.1$ . We have again used  $\mathcal{O}_+$  as the operator coupling to the impurity potential. The plots are significantly different and less universal than the vanishing charge density case, of figure 4. As  $\rho$  becomes nonzero, a local maximum appears at small temperatures and moves rapidly to the right as the charge density is increased. Note that unlike the  $\rho = 0$  case we considered previously, plot 5a in particular is vulnerable to the unknown  $\bar{V}^2 B^2$  corrections to  $\gamma$  that we mentioned in section 3.2 above. Its qualitative form however should be correct, as it needs to interpolate between figures 4 and 5b.

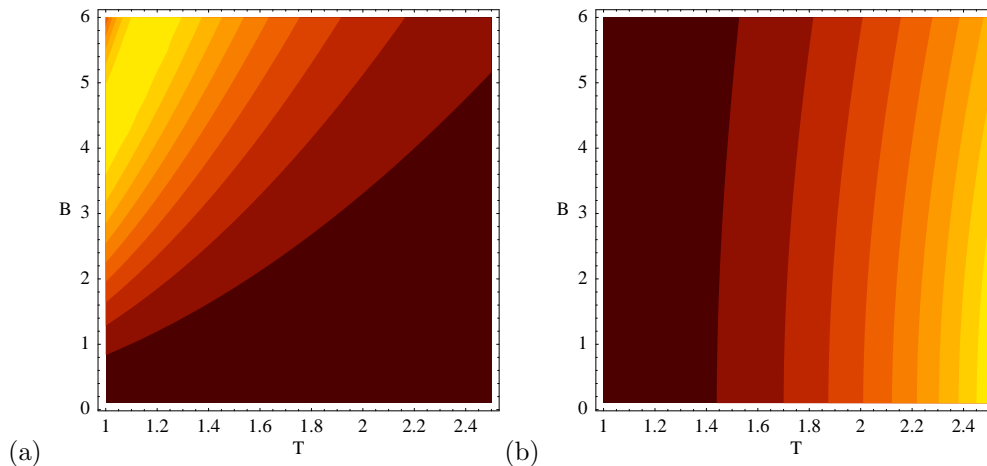


Figure 5: The Nernst signal  $N$  for the truncated M2 brane theory as a function of  $B$  and  $T$ , with (a) charge density  $\rho/\sigma_0 = 8.3 \times 10^{-5}$  and (b) charge density  $\rho/\sigma_0 = 10$ , and  $\bar{V} = 0.1$  in both cases. The impurity potential is coupled to  $\mathcal{O}_+$ . Lighter denotes a larger Nernst coefficient.

What we learn from these plots is that (with  $\bar{V} = 0.1$ ) a very small  $\rho/\sigma_0 \sim 10^{-5}$  is already sufficient to produce significant deviations from the  $\rho = 0$  result. This suggests that one would have to tune very close to the insulating doping of  $x_I = 1/8$  in order to see the scaling  $\rho = 0$  behaviour of equation (65). However, it is curious that the observations in [34] do appear to show similar behaviour at low  $B$  and with  $T$  just above  $T_c$ .

## 7 Discussion

### 7.1 Summary of results for the impure CFT

In this paper we have derived a general formula (12) for the impurity relaxation timescale at a quantum critical point. Some of our steps in section 3 were adapted from earlier works [24, 25, 26].

We then used our formula to obtain  $\tau_{\text{imp}}$  for the truncated M2 brane theory. We found that there were two relevant operators  $\mathcal{O}_{\pm}$  that were neutral under a global  $U(1)$  symmetry. This led to the following results

- For the ‘magnetic’ operator dual to the scalar field  $\psi_+$ , increasing the magnetic field  $B$  and charge density  $\rho$  suppresses momentum relaxation due to impurities, see figure 1a. At small  $B$  and sufficiently large  $\rho$ , this implies that the cyclotron resonance described in [8, 9] may be easier to observe experimentally than previously estimated because the impurity damping effects become smaller.
- For the operator dual to the scalar field  $\psi_-$ , in contrast, the inverse relaxation time increases when the charge density  $\rho$  and magnetic field  $B$  are increased. Beyond the critical value  $\mathcal{Q} = \sqrt{B^2 + \rho^2/\sigma_0^2} \approx 21T^2$ , the inverse relaxation time actually diverges. See figure 1b. We saw that the divergence is associated with a new instability in the underlying finite temperature CFT. The scalar field  $\psi_-$  develops an unstable mode when the  $\mathcal{Q}$  gets too large. This instability is dual to a phase transition to an ordered state in which  $\mathcal{O}_-$  condenses.
- The Nernst coefficient for the truncated M2 brane theory with vanishing charge density,  $\rho = 0$ , is shown in figure 4 with impurity relaxation due to the  $\mathcal{O}_+$  operator. We noted that our dependence on  $T$  and  $B$  is qualitatively similar to the results for low magnetic fields and for temperature close to the critical temperature observed in various types of superconductors [18, 34, 35]. This comparison makes most sense for the data in [18], in which the system is not doped. It is interesting to note, however, the similarity in the Nernst response between the different superconductors in this regime.

## 7.2 Some directions for future work

Our results are perturbative in the strength of the impurity potential  $\bar{V}$  and valid at high temperatures. We furthermore used the memory function formalism, which requires  $1/\tau_{\text{imp}}$  not to be too large. Various techniques have been developed in condensed matter theory for treating random disorder more exactly. It would be very interesting to see if these can be applied to the M2 brane theory.

Our treatment of the M2 brane theory was not completely satisfactory. We made an inconsistent truncation in order to avoid dealing with more than one  $U(1)$  gauge field. We also made a nonconventional choice for the conformal dimension of our supergravity mode  $\chi$ . One clear project for the future is to repeat the calculations presented here including the extra  $U(1)$  gauge field and using the standard choice of conformal dimension for  $\chi$ .

But it would also be interesting to take a more general approach. While in our M2 brane theory, the operators we considered had conformal dimension  $\Delta_{\mathcal{O}} = 1$ , in general the spectrum of operator dimensions will depend on the CFT. Our bulk equation of motion (44) for the scalar field  $\phi$  dual to the operator  $\mathcal{O}$  can be generalised to allow the scalar field to have an arbitrary mass. This is dual to allowing  $\Delta_{\mathcal{O}}$  to vary. One could imagine using the AdS/CFT correspondence more ‘phenomenologically’ to see how the effects of impurity relaxation depend on the dimension of  $\mathcal{O}$ .

One result of this paper is the instability of the truncated M2 brane theory at  $\sqrt{B^2 + \rho^2/\sigma_0^2} \approx 21T^2$ . We noted that this instability is a counterexample to the original formulation of the correlated stability conjecture, as the black hole is thermodynamically stable at this value of the charge density and magnetic field. As with the previously studied counterexamples [17], the mismatch between

dynamics and thermodynamics occurs because there is no conserved charge associated with the scalar fields. The instability presumably indicates the existence of new dyonic black hole solutions in which both the scalar  $\phi$  and pseudoscalar  $\chi$  are nonvanishing. It would be interesting to find these new solutions and understand their implications for the dual theory.

In combining the effects of impurities and an external magnetic field, we were constrained to work in a regime where  $B/T^2$  was not too large. It would be nice to relax this requirement. An approach via Ward identities looks promising.

We have noted that the Nernst effect in systems with vanishing charge density can be a very clean indicator of the proximity of a quantum critical point, via the scaling relation (65). Perhaps this scaling can be searched for in future measurements of the Nernst effect.

## Acknowledgements

We would like to thank Ofer Aharony, David Berenstein, Steve Gubser, David Huse, Igor Klebanov, Nai-Phuan Ong, Joe Polchinski and Antonello Scardicchio for valuable discussions. We would also like to thank Subir Sachdev and Markus Mueller for helpful correspondence. SAH thanks the Weizmann Institute for hospitality while this work was being completed. This work was supported in part by the National Science Foundation (NSF) under Grants No. PHY-0243680 and PHY05-51164. Any opinions, findings, and conclusions or recommendations expressed in this material are those of the authors and do not necessarily reflect the views of the NSF.

## A Relating $G_{\mathcal{PP}}^R$ to a conductivity

The connection between  $G_{\mathcal{PP}}^R(\omega, 0)$  and  $\theta$  is established as follows. The momentum conductivity is defined by

$$\langle \mathcal{P} \rangle = -\theta(\omega, 0) \nabla T. \quad (69)$$

The momentum density  $\mathcal{P}$  can be sourced by fluctuating the background spacetime metric. Specifically, by definition there is a coupling between metric fluctuations and the stress tensor in the action,  $\delta S = \frac{1}{2} \int d^3x T^{\mu\nu} \delta g_{\mu\nu}$ . (We are treating  $T^{\mu\nu}$  as a tensor density rather than a tensor field and hence have absorbed a factor of  $\sqrt{-g}$ .) Without loss of generality by rotation invariance, we can restrict to a fluctuation only in the spatial direction  $\delta g_{0i}$ . Choosing  $n^j = \delta_{ij}$ , linear response theory then implies

$$\langle \mathcal{P} \rangle = G_{\mathcal{PP}}^R(\omega, 0) \delta g_{0j} n^j. \quad (70)$$

The remaining step is to show that  $\delta g_{0i}$  is gauge equivalent to a thermal gradient. Recall that under a diffeomorphism generated by the vector  $\xi^a$ , metric perturbations transform as  $\delta g_{ab} = \partial_a \xi_b + \partial_b \xi_a$ . We choose  $\xi_i = 0$  and  $\partial_i \xi_0 = -\delta g_{0i}$ . After this gauge transformation  $\delta g_{0i}$  vanishes and  $\partial_i \delta g_{00} = 2i\omega \delta g_{0i}$ , assuming the fluctuations have a time dependence of the form  $e^{-i\omega t}$ . Recall that the Euclidean time direction is periodic with period  $1/T$ . It is convenient to fix the period and take  $g_{00} = 1/T^2$ . A shift in temperature thus implies  $\partial_i g_{00} = -2\partial_i T/T^3 = -2g_{00} \partial_i T/T$ , to leading order in  $\partial_i T$ . Putting these formulae together leads to the intermediate result

$$\delta g_{0i} = -\frac{g_{00} \partial_i T}{i\omega T}. \quad (71)$$

We have to be careful in interpreting this result because we rescaled time at an intermediate step. Moreover, we rescaled  $g_{00}$  without rescaling  $\omega$ . We now need to rescale time back to the lab frame,

where time has period  $1/T$  in the Euclidean direction, being careful not to rescale  $\omega$ :

$$\delta g_{0i} = -\frac{\partial_i T}{i\omega T} . \quad (72)$$

Thus we find from (69) and (70) that

$$i\theta(\omega, 0)T\omega \equiv G_{\mathcal{PP}}^R(\omega, 0) , \quad (73)$$

as claimed in the main text. As we noted,  $G_{\mathcal{PP}}^R(\omega, 0)$  needs to be corrected by a contact term to give a sensible  $\omega \rightarrow 0$  limit for the conductivity.

## B Hydrodynamics and the memory method

In this appendix we show that the results obtained from hydrodynamics in [9] and [8] are completely consistent with the memory function methods. Consider  $G_{\mathcal{JJ}}^R \equiv \omega\sigma_+$  for the choice  $n_i = (1, -i)/\sqrt{2}$ . We will henceforth suppress the superscript  $R$  since it is clear we work only with retarded Green's functions in this appendix. In [9], for a translationally invariant theory in the hydrodynamic limit, it was argued that this holomorphic conductivity takes the form

$$\sigma_+ = i\sigma \frac{\omega + i\omega_c^2/\gamma + \omega_c}{\omega + i\gamma - \omega_c} . \quad (74)$$

Using (25), we find that

$$G_{\mathcal{PP}}(\omega) = (\epsilon + P) \frac{i\gamma - \omega_c}{\omega + i\gamma - \omega_c} . \quad (75)$$

As expected,  $G_{\mathcal{PP}}(0) = \epsilon + P = \chi_0$ . Moreover, this result is entirely consistent with the memory function formalism,

$$\lim_{B \rightarrow 0} \frac{\omega G_{\mathcal{PP}}(\omega)}{\chi_0} = i\gamma - \omega_c . \quad (76)$$

This limit is  $B/T^2 \rightarrow 0$ . The frequency  $\omega/T$  is kept small but fixed.

In [8], it was shown that an impurity scattering time could be introduced by making the replacement  $\omega \rightarrow \omega + i/\tau$  in the conductivities. This followed from hydrodynamics plus a relaxation of momentum imposed by hand. This substitution yields

$$\sigma'_+ = i\sigma \frac{\omega + i/\tau + i\omega_c^2/\gamma + \omega_c}{\omega + i/\tau + i\gamma - \omega_c} . \quad (77)$$

which agrees with the combination  $\sigma_{xy} + i\sigma_{xx}$  from [8]. We use the superscript  $'$  to indicate a Green's function or conductivity in the presence of impurities. The prescription is trickier when applied to  $G_{\mathcal{PP}}$ . The relevant transport coefficient we will call  $\theta_+$  is related via  $\omega T\theta_+ = G_{\mathcal{PP}}(\omega) - \chi_0$ . Thus

$$\theta'_+ T = -\frac{\chi_0}{\omega + i/\tau + i\gamma - \omega_c} , \quad (78)$$

which then implies that

$$G'_{\mathcal{PP}}(\omega) = \chi_0 \frac{i/\tau + i\gamma - \omega_c}{\omega + i/\tau + i\gamma - \omega_c} . \quad (79)$$

Again, the memory function method works with this modified  $G'_{\mathcal{PP}}$  yielding a pole at the appropriate  $\omega = -i/\tau - i\gamma + \omega_c$ .

Let's now compute

$$B^2(\sigma'_+(\omega) - \sigma_+(0)) = \chi_0 \frac{(\omega + i/\tau)(i\gamma - \omega_c)}{(\omega + i/\tau + i\gamma - \omega_c)} , \quad (80)$$

and check the extent to which (25) continues to hold in the small  $1/\tau$  and  $B$  limit:

$$\lim_{B, \frac{1}{\tau} \rightarrow 0} \frac{\omega}{\chi_0} \left( G'_{\mathcal{PP}}(\omega) - \frac{B^2}{\omega^2} (G'_{\mathcal{JJ}}(\omega) - G_{\mathcal{JJ}}(0)) \right) = i\gamma - \omega_c + i/\tau - (i\gamma - \omega_c) = i/\tau. \quad (81)$$

Indeed, that's exactly the result we were looking for, suggesting (29) is correct. We have made only an indirect assumption about the  $B$  dependence of  $1/\tau$ . Our hydrodynamic framework is valid only up to  $\mathcal{O}(B^2)$ . Thus while (22) appears to capture the full  $B$  dependence of  $1/\tau$ , in this hydrodynamic context, we can trust the answer only up to  $\mathcal{O}(B^2)$ .

## C Action for fluctuations without truncation

In this appendix we give, for possible future use, the untruncated action for perturbations of the dyonic black hole background (34) and (35).

From appendix F of [29] one can check that the full action for 3 scalars, 3 pseudoscalars and 4 gauge fields may be consistently truncated for linearised perturbations of the dyonic black hole to one scalar,  $\phi$ , one pseudoscalar,  $\chi$ , and one gauge field  $G$ :

$$\begin{aligned} S = -\frac{1}{2\kappa_4^2} \int d^4x \sqrt{-g} \quad & \left( R - \frac{1}{2} [(\partial_\mu \phi)(\partial^\mu \phi) + (\partial_\mu \chi)(\partial^\mu \chi)] + 2L^{-2} [3 + \frac{1}{2}(\phi^2 + \chi^2)] \right. \\ & - L^2 [1 + \frac{1}{2}(\phi^2 - \chi^2)] F_{\mu\nu} F^{\mu\nu} + \frac{1}{2} L^2 \phi \chi \epsilon^{\mu\nu\rho\sigma} F_{\mu\nu} F_{\rho\sigma} \\ & \left. - L^2 G_{\mu\nu} G^{\mu\nu} - 2L^2 \phi F_{\mu\nu} G^{\mu\nu} + L^2 \chi \epsilon^{\mu\nu\lambda\rho} F_{\mu\nu} G_{\lambda\rho} \right). \end{aligned} \quad (82)$$

We have used the same notation as in the main text. In particular  $G_{\mu\nu} = \delta F_{\mu\nu}^{(1)} + \delta F_{\mu\nu}^{(2)} - \delta F_{\mu\nu}^{(3)} - \delta F_{\mu\nu}^{(4)}$ , whereas the background gauge field is  $F_{\mu\nu} = F_{\mu\nu}^{(1)} + F_{\mu\nu}^{(2)} + F_{\mu\nu}^{(3)} + F_{\mu\nu}^{(4)}$ .

Once again it is useful to introduce the fields  $\psi_\pm$  defined in (40). Evaluated on the dyonic black hole background, the action becomes

$$S = -\frac{1}{2\kappa_4^2} \int d^4x \sqrt{-g} \quad \left( -\frac{1}{2} [(\partial_\mu \psi_+)(\partial^\mu \psi_+) + (\partial_\mu \psi_-)(\partial^\mu \psi_-)] + L^{-2} (\psi_+^2 + \psi_-^2) \right) \quad (83)$$

$$-L^{-2} z^4 (h^2 + q^2) (\psi_+^2 - \psi_-^2) - L^2 G_{\mu\nu} G^{\mu\nu} \quad (84)$$

$$-4L^{-2} \frac{z^4}{\alpha^2} \sqrt{h^2 + q^2} (\alpha \psi_- G_{tz} + \psi_+ G_{xy}) \Big). \quad (85)$$

In this expression we note that once again the background magnetic and electric charges only appear in the combination  $h^2 + q^2$ . It should be possible to decouple the equations of motion following from this action and find the momentum relaxation in the full theory. Solving the full equations would also be of interest in terms of revisiting the computations in [15, 16].

## D Exponential falloff at large $k$

The exponential falloff of the imaginary part of the Green's function with large spatial momentum  $k$  can be seen from a WKB analysis. To perform a WKB analysis of the differential equation (44), we first transform it into Schrodinger form. (A very similar analysis was performed in an appendix of ref. [27].) To that end, we define a new wavefunction  $\Phi_\pm$  such that  $\Phi_\pm(\rho) = \psi_\pm(z)/z$  and a new radial coordinate  $\rho(z)$  such that  $\partial_z \rho = 1/f$ . With these new definitions, the differential equation becomes

$$(-\partial_\rho^2 + V(\rho) - \mathfrak{w}^2) \Phi_\pm(\rho) = 0 \quad (86)$$



where

$$V(\rho) = \frac{f}{z^2}(m^2 L^2 + \mathfrak{q}^2 z^2 + 2f - z\partial_z f \pm 2z^4(q^2 + h^2)) . \quad (87)$$

In terms of the new radial variable, we can take

$$\rho = \int_0^z \frac{dz'}{f(z')} . \quad (88)$$

Thus, the horizon at  $z_h = 1$  has been moved to  $\rho_h \rightarrow \infty$ . The boundary at  $z_b = 0$  remains at  $\rho_b = 0$ .

Note that for  $m^2 L^2 = -2$  we have  $V(0) = \mathfrak{q}^2$ . We are interested in the case of spacelike momentum,  $k \gg \omega$ , for which there are no classical turning points. The wavefunction is exponentially damped everywhere. The imaginary part of the retarded Green's function will be proportional to the probability for the particle to reach the horizon at  $z_h = 1$ :

$$\text{Im } G_{\mathcal{O}\mathcal{O}}^R \sim \exp\left(-2 \int_0^\infty d\rho \sqrt{V(\rho) - \mathfrak{w}^2}\right) . \quad (89)$$

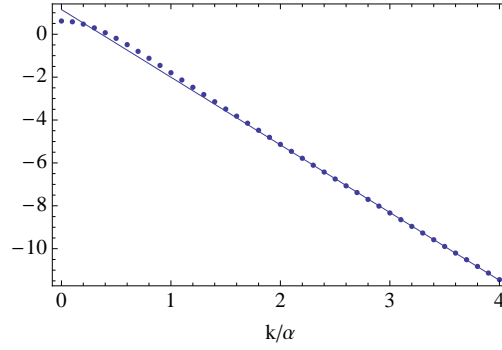


Figure 6: The points are numerically determined values of the log of the imaginary part of  $G_{\mathcal{O}\mathcal{O}}^R(0, k)$  as a function of  $k$  for  $q^2 + h^2 = 1/4$  and the  $\psi_+$  scalar field. More specifically, we plot  $\ln(\lim_{\mathfrak{w} \rightarrow 0} B/\mathfrak{w}A)$ . The line is a best fit  $1.15 - 3.15\mathfrak{q}$ . For these values of  $q$  and  $h$ , WKB gives us  $a = 2.86$ .

Given that  $k \gg \omega$ , we can approximately evaluate this integral to give  $\text{Im } G_{\mathcal{O}\mathcal{O}}^R \sim \exp(-ak/\alpha)$  where we have defined the coefficient

$$a \equiv 2 \int_0^1 \frac{dz}{\sqrt{f(z)}} . \quad (90)$$

In other words, the WKB analysis is telling us that  $\text{Im } G_{\mathcal{O}\mathcal{O}}^R$  is exponentially damped for large enough  $k/\alpha$ . In the case where  $h = q = 0$ , we may evaluate the integral analytically to find

$$\int_0^1 \frac{dz}{\sqrt{1 - z^3}} = \frac{\sqrt{\pi}\Gamma(4/3)}{\Gamma(5/6)} \approx 1.402 . \quad (91)$$

In order for our integral (52) over  $\mathfrak{q} = k/\alpha$  of the imaginary part of the Green's function to converge, this exponential damping is important. We observed it numerically for more general values of  $h$  and  $q$ . In Figure 6, we plot the log of the imaginary part of  $G_{\mathcal{O}\mathcal{O}}^R(0, k)$  as a function of  $k/\alpha$  and indeed see linear behavior at large  $k$ .

## References

- [1] S. Sachdev, *Quantum Phase Transitions*, CUP, 1999.
- [2] S. Sachdev, “Quantum magnetism and criticality”, arXiv:0711.3015 [cond-mat.str-el].
- [3] J. M. Tranquada, B. J. Sternlieb, J. D. Axe, Y. Nakamura and S. Uchida, “Evidence for stripe correlations of spins and holes in copper oxide superconductors,” *Nature* **375** (1995) 561.
- [4] S. Sachdev, “Order and quantum phase transitions in the cuprate superconductors,” *Rev. Mod. Phys.* **75** (2003) 913.
- [5] J. M. Maldacena, “The large N limit of superconformal field theories and supergravity,” *Adv. Theor. Math. Phys.* **2** (1998) 231 [*Int. J. Theor. Phys.* **38** (1999) 1113] [arXiv:hep-th/9711200].
- [6] C. P. Herzog, P. Kovtun, S. Sachdev and D. T. Son, “Quantum critical transport, duality, and M-theory,” *Phys. Rev. D* **75** (2007) 085020, [arXiv:hep-th/0701036].
- [7] S. A. Hartnoll and P. Kovtun, “Hall conductivity from dyonic black holes,” *Phys. Rev. D* **76** (2007) 066001, [arXiv:0704.1160 [hep-th]].
- [8] S. A. Hartnoll, P. K. Kovtun, M. Muller and S. Sachdev, “Theory of the Nernst effect near quantum phase transitions in condensed matter, and in dyonic black holes,” *Phys. Rev. B* **76** (2007) 144502, [arXiv:0706.3215 [cond-mat.str-el]].
- [9] S. A. Hartnoll and C. P. Herzog, “Ohm’s Law at strong coupling: S duality and the cyclotron resonance,” *Phys. Rev. D* **76** (2007) 106012, [arXiv:0706.3228 [hep-th]].
- [10] C. P. Herzog, “The hydrodynamics of M-theory,” *JHEP* **0212** (2002) 026, [arXiv:hep-th/0210126].
- [11] C. P. Herzog, “The sound of M-theory,” *Phys. Rev. D* **68** (2003) 024013, [arXiv:hep-th/0302086].
- [12] O. Saremi, “The viscosity bound conjecture and hydrodynamics of M2-brane theory at finite chemical potential,” *JHEP* **0610** (2006) 083, [arXiv:hep-th/0601159].
- [13] E. Witten, “Multi-trace operators, boundary conditions, and AdS/CFT correspondence,” arXiv:hep-th/0112258.
- [14] O. Aharony, S. S. Gubser, J. M. Maldacena, H. Ooguri and Y. Oz, “Large N field theories, string theory and gravity,” *Phys. Rept.* **323** (2000) 183, [arXiv:hep-th/9905111].
- [15] S. S. Gubser and I. Mitra, “The evolution of unstable black holes in anti-de Sitter space,” *JHEP* **0108** (2001) 018 [arXiv:hep-th/0011127].
- [16] S. S. Gubser and I. Mitra, “Instability of charged black holes in anti-de Sitter space,” arXiv:hep-th/0009126.
- [17] J. J. Friess, S. S. Gubser and I. Mitra, “Counter-examples to the correlated stability conjecture,” *Phys. Rev. D* **72**, 104019 (2005) [arXiv:hep-th/0508220].
- [18] M-S. Nam, A. Ardavan, S. J. Blundell and J. A. Schlueter, “Fluctuating superconductivity in organic molecular metals close to the Mott transition,” *Nature* **449** (2007) 584.

- [19] A. Altland and B. Simons, *Condensed matter field theory*, Cambridge University Press, 2006.
- [20] J. Cardy, *Scaling and Renormalization in Statistical Physics*, Cambridge University Press, 1996.
- [21] O. Aharony, Y. Oz and Z. Yin, “M-theory on  $\text{AdS}(p) \times \text{S}(11-p)$  and superconformal field theories,” *Phys. Lett. B* **430** (1998) 087, [arXiv:hep-th/9803051].
- [22] S. Minwalla, “Particles on  $\text{AdS}(4/7)$  and primary operators on  $\text{M}(2/5)$  brane worldvolumes,” *JHEP* **9810** (1998) 002, [arXiv:hep-th/9803053].
- [23] E. Halyo, “Supergravity on  $\text{AdS}(4/7) \times \text{S}(7/4)$  and M branes,” *JHEP* **9804** (1998) 011, [arXiv:hep-th/9803077].
- [24] W. Götze and P. Wolfle, “Homogeneous dynamical conductivity of simple metals,” *Phys. Rev.* **B6** (1972) 1226.
- [25] T. Giamarchi, “Umklapp process and resistivity in one-dimensional fermion systems,” *Phys. Rev.* **B44** (1991) 2905.
- [26] P. N. Argyres and D. G. Resendes, “Discussion of the memory-function method,” *J. Phys: Condens. Matter* **1** (1989) 7001.
- [27] D. T. Son and A. O. Starinets, “Minkowski-space correlators in  $\text{AdS/CFT}$  correspondence: Recipe and applications,” *JHEP* **0209** (2002) 042, [arXiv:hep-th/0205051].
- [28] M. J. Duff and J. T. Liu, “Anti-de Sitter black holes in gauged  $N = 8$  supergravity,” *Nucl. Phys. B* **554** (1999) 237, [arXiv:hep-th/9901149].
- [29] M. J. Duff, “Lectures on branes, black holes and anti-de Sitter space,” arXiv:hep-th/9912164.
- [30] C. Erginsoy, “Neutral Impurity Scattering in Semiconductors,” *Phys. Rev.* **79** (1950) 1013.
- [31] I. R. Klebanov and E. Witten, “ $\text{AdS/CFT}$  correspondence and symmetry breaking,” *Nucl. Phys. B* **556** (1999) 089, [arXiv:hep-th/9905104].
- [32] Z. A. Xu, N. P. Ong, Y. Wang, T. Kakeshita and S. Uchida, “Vortex-like excitations and the onset of superconducting phase fluctuation in underdoped  $\text{La}_{2-x}\text{Sr}_x\text{CuO}_4$ ,” *Nature* **406** (2000) 486.
- [33] A. Pourret, H. Aubin, J. Lesueur, C. A. Marrache-Kikuchi, L. Berge, L. Dumoulin and K. Behnia, “Observation of the Nernst signal generated by fluctuating Cooper pairs,” *Nature Physics* **2** (2006) 683.
- [34] Y. Wang, L. Li and N. P. Ong, “Nernst effect in high- $T_c$  superconductors,” *Phys. Rev.* **B73** (2006) 024510.
- [35] A. Pourret, H. Aubin, J. Lesueur, C. A. Marrache-Kikuchi, L. Berge, L. Dumoulin and K. Behnia, “A length scale for the superconducting Nernst signal above  $T_c$  in  $\text{Nb}_{0.15}\text{Si}_{0.85}$ ,” arXiv:cond-mat/0701376.
- [36] A. V. Balatsky and P. Bourges, “Linear dependence of peak width in  $\chi(q, \omega)$  vs  $T_c$  for YBCO superconductors,” *PRL* **82** (1999) 5337.
- [37] Y. Liu and A. M. Goldman, “Superconductor-insulator transitions in two dimensions,” *Mod. Phys. Lett* **B8** (1994) 277.